Biomedical Materials

PAPER

Adult skin-derived precursor Schwann cell grafts form growths in the injured spinal cord of Fischer rats

Zacnicte May[1] , Ranjan Kumar[2], Tobias Fuehrmann[3] , Roger Tam[3], Katarina Vulic[3], Juan Forero[1], Ana Lucas Osma[1], Keith Fenrich[1], Peggy Assinck[4,5], Michael J Lee[4], Aaron Moulson[4,6], Molly S Shoichet[3] , Wolfram Tetzlaff[4,6,7], Jeff Biernaskie[2] and Karim Fouad[1]

[1] Department of Physical Therapy, Faculty of Rehabilitation Medicine, and Neuroscience and Mental Health Institute, University of Alberta, Edmonton, AB, T6G 2E1, Canada
[2] Department of Comparative Biology and Experimental Medicine, Faculty of Veterinary Medicine, Alberta Children's Hospital Research Institute, University of Calgary, Calgary, Alberta, AB, Canada
[3] Department of Chemical Engineering & Applied Chemistry, Department of Chemistry, Institute of Biomaterials and Biomedical Engineering, University of Toronto, Toronto, ON M5S 3E1, Canada
[4] International Collaboration on Repair Discoveries, University of British Columbia, Vancouver, British Columbia, V6T 1Z4, Canada
[5] Graduate Program in Neuroscience, University of British Columbia, Vancouver, British Columbia, V6T 1Z4, Canada
[6] Department of Zoology, University of British Columbia, Vancouver, British Columbia, V6T 1Z4, Canada
[7] Department of Surgery, University of British Columbia, Vancouver, British Columbia, V6T 1Z4, Canada

E-mail: karim.fouad@ualberta.ca

Abstract

In this study, GFP$^+$ skin-derived precursor Schwann cells (SKP-SCs) from adult rats were grafted into the injured spinal cord of immunosuppressed rats. Our goal was to improve grafted cell survival in the injured spinal cord, which is typically low. Cells were grafted in hyaluronan-methylcellulose hydrogel (HAMC) or hyaluronan-methylcellulose modified with laminin- and fibronectin-derived peptide sequences (eHAMC). The criteria for selection of hyaluronan was for its shear-thinning properties, making the hydrogel easy to inject, methylcellulose for its inverse thermal gelation, helping to keep grafted cells *in situ*, and fibronectin and laminin to improve cell attachment and, thus, prevent cell death due to dissociation from substrate molecules (i.e., anoikis). Post-mortem examination revealed large masses of GFP$^+$ SKP-SCs in the spinal cords of rats that received cells in HAMC (5 out of $n = 8$) and eHAMC (6 out of $n = 8$). Cell transplantation in eHAMC caused significantly greater spinal lesions compared to lesion and eHAMC only control groups. A parallel study showed similar masses in the contused spinal cord of rats after transplantation of adult GFP$^+$ SKP-SCs without a hydrogel or immunosuppression. These findings suggest that adult GFP$^+$ SKP-SCs, cultured/transplanted under the conditions described here, have a capacity for uncontrolled proliferation. Growth-formation in pre-clinical research has also been documented after transplantation of: human induced pluripotent stem cell-derived neural stem cells (Itakura *et al* 2015 *PLoS One* **10** e0116413), embryonic stem cells and embryonic stem cell-derived neurons (Brederlau *et al* 2006 *Stem Cells* **24** 1433–40; Dressel *et al* 2008 *PLoS One* **3** e2622), bone marrow derived mesenchymal stem cells (Jeong *et al* 2011 *Circ. Res.* **108** 1340–47) and rat nerve-derived SCs following *in vitro* expansion for >11 passages (Funk *et al* 2007 *Eur. J. Cell Biol.* **86** 207–19; Langford *et al* 1988 *J. Neurocytology* **17** 521–9; Morrissey *et al* 1991 *J. Neurosci.* **11** 2433–42). It is of upmost importance to define the precise culture/transplantation parameters for maintenance of normal cell function and safe and effective use of cell therapy.

1. Introduction

Spinal cord injury (SCI) is a devastating event because it results in partial to complete loss of sensory and motor function below the level of injury and secondary complications, such as pain and autonomic dysfunction. In the United States, there are ~282 000 persons living with SCI with 17 000 new cases every year

(National Spinal Cord Injury Statistical Center 2016), and there is no robust treatment to reliably promote recovery. The complexity of SCI pathophysiology (reviewed in Hagg and Oudega 2006) explains, in part, the relative absence of effective treatments. Axons are unable to regenerate into and beyond the site of SCI due to lack of growth-promoting molecules (Pearse *et al* 2004), various inhibitors to axonal regeneration (Fawcett and Asher 1999, Cafferty *et al* 2010), and the formation of a fluid-filled cavity at the injury epicenter, creating a need for a substrate for growing axons (Oudega *et al* 2012). Therefore, grafting cells to create a bridge across the lesion cavity is a frequently attempted avenue. In particular, Schwann cell (SC) grafts have been shown to provide a supportive growth substrate for axons (Bunge 1975, Richardson *et al* 1980, Oudega and Xu 2006, Tetzlaff *et al* 2011, Williams *et al* 2015), and release a host of axon growth-promoting factors, including NGF, BDNF, and NT-3 (Meyer *et al* 1992, Funakoshi *et al* 1993, Meier *et al* 1999, Sahenk *et al* 2008, Richner *et al* 2014). SCs are also involved in myelinating spared and regenerating axons (McKenzie *et al* 2006, Biernaskie *et al* 2007b, Xu and Onifer 2009). One obstacle in the use of SCs is boundary formation between SCs and astrocytes, preventing SC graft integration within the injured CNS (Franklin and Barnett 1997). Thus, it has been argued that oligodendrocytes or olfactory ensheathing cells (OECs) might be more suitable candidates for transplantation. However, myelin-associated molecules produced by oligodendrocytes have an inhibitory effect on axonal regeneration (Bandtlow *et al* 1990, Chen *et al* 2000, Wang *et al* 2002). Similar to SCs, OECs re-myelinate demyelinated axons and support axonal regeneration (Franklin and Barnett 1997, Barnett and Riddell 2004) but have a number of drawbacks, such as small yield of OECs from human nasal mucosa (Choi *et al* 2008) and challenges in purification and characterization of OEC cultures (Kawaja *et al* 2009).

Although multiple pre-clinical studies suggested that SC transplantation following SCI translates into modest functional recovery (Sharp *et al* 2012, Flora *et al* 2013, Williams *et al* 2015), it is generally accepted that in order for SCs to be effective in restoring function combinatory approaches (e.g., pro-regenerative treatments in addition to the cell grafts) are needed (Fouad *et al* 2005, Oudega and Xu 2006, Oudega*et al* 2012). Because of the potential beneficial effects there are on-going clinical trials testing the safety of grafting SCs in humans with SCI (http://clinicaltrials.gov/ct2; NCT02354625; NCT01739023).

Despite the multitude of studies on SC grafts, many basic questions about SC therapy remain unanswered, including the best source of SCs (Tetzlaff *et al* 2011). Typically, SCs for cell transplantation are obtained from samples of peripheral nerve (Murray and Stout 1942, Bunge 1975, Pearse *et al* 2004, Fouad *et al* 2005, Williams *et al* 2015). An alternative source is the skin dermis, which contains multipotent progenitor cells called skin-derived precursors (SKPs; Toma *et al* 2001, Joannides *et al* 2004, Toma *et al* 2005) that can be successfully differentiated into SCs (McKenzie *et al* 2006, Biernaskie *et al* 2007a, 2007b). SKPs are cultured as floating spheres and differentiated into SCs by removing fibroblast growth factor 2 and epidermal growth factor from cell culture media and adding neuregulin (Biernaskie *et al* 2007a). Skin biopsies as compared to nerve are less invasive and do not result in significant morbidity as a consequence of nerve resection (Biernaskie *et al* 2007a) making SKP-SCs a highly accessible, autologous source of SCs for cell therapy. In tissue culture, neonatal and adult SKP-SCs survive well, display a bipolar morphology as seen with nerve-derived SCs, express p75, S100, and GFAP, all common markers of SCs, and can be purified to >95% purity (Biernaskie *et al* 2007a).

Survival of grafted SCs in the injured spinal cord is a major challenge. Survival rates of peripheral nerve-derived SCs 6–9 weeks post-transplantation range from 1% to 20% (Golden *et al* 2007, Pearse *et al* 2007, Enomoto *et al* 2013) and survival rates of SKP-SCs 11 weeks post-transplantation are ~18% (Biernaskie *et al* 2007b). One of the causes of SC loss post-transplantation is immune-mediated rejection. In fact, immuno-suppression with cyclosporine has been reported to increase SC survival in the injured rat spinal cord (Hill *et al* 2006). A second cause of SC loss is anoikis (Koda *et al* 2008), a type of apoptosis due to detachment of cells from the extracellular matrix (ECM) and surrounding cells (Frisch and Francis 1994). These factors need to be addressed in pre-clinical research to maximize survival of grafted cells.

In the present study, we attempted to promote the survival of grafted SKP-SCs in order to create a bridge for regenerating axons in future combinatory treatments. Criteria for successful grafts include: survival of >25% of originally grafted cells (a survival rate of ~18% has previously been reported by Biernaskie *et al* 2007b), filling of the SCI site with SKP-SCs, and possibly axonal growth into the graft (as seen in Biernaskie *et al* 2007b). To achieve this goal, SKP-SCs were grafted in hydrogel rather than media, since the increased viscosity of hydrogels prevents injected cells from spreading and localizes cells to the injection site (Ballios *et al* 2010, 2015). Tighter clustering of grafted cells due to hydrogels' viscosity was also anticipated to prevent anoikis. Two different hydrogels were used: a blend of hyaluronan (HA) and methylcellulose (MC) called HAMC and a peptide modified HAMC (eHAMC). HAMC was used, because it has recently shown promise in the field of SCI by reducing inflammation (Austin *et al* 2012), which could result in enhanced cell survival. Furthermore, HAMC is easily injectable due to the shear thinning properties of HA and the inverse thermal gelling properties of MC (Gupta *et al* 2006). For eHAMC, laminin and fibronectin-derived peptide sequences were conjugated to

MC (Mothe *et al* 2013). Laminin and fibronectin peptides are important molecules in the ECM involved in cell attachment (Baron-Van Evercooren *et al* 1982, Tohyama and Ide 1984). Therefore, this latter formulation was expected to further reduce cell spreading and anoikis by providing ECM attachment molecules. As a final measure to ensure grafted cell survival, rats were immunosuppressed with cyclosporine. In sum, our goal was to maximize SKP-SC survival within the SCI cavity by preventing grafted cell spreading and anoikis with HAMC hydrogels and preventing graft rejection with cyclosporine.

We report on a second adult SKP-SC transplantation experiment without the use of hydrogels or immune suppression. We refer to the first transplantation experiment as the 'SKP-SCs in hydrogel study' and the second experiment as the 'SKP-SCs in media study' throughout the article. The two studies were conducted in parallel but were never intended to be compared directly. In the SKP-SCs in hydrogel study, the SCI model was a hemi-section, SKP-SCs were transplanted in HAMC hydrogel, rats were immunosuppressed, and female rats were used. In contrast, in the SKP-SCs in media study a hemi-contusion SCI model was used, SKP-SCs were transplanted in media, rats were not immunosuppressed, and male rats were used. However, formation of detrimental masses/growths of transplanted SKP-SCs was observed in both studies. Hence, the parallel studies were included to exhibit growth-formation post-transplantation of adult SKP-SCs despite wide differences in methodology, showing growth formation may occur independent of these methodological differences.

2. Materials and methods

2.1. Animals

SKP-SCs in hydrogel: Adult female Fischer (CDF®) rats ($N = 20$; Charles River Laboratories, Wilmington, MA, USA) weighing between 161 and 182 g were housed in groups of five rats per large ($18'' \times 14''$) cage under a 12:12 h light-dark cycle. Rats were acclimatized for 1 week before starting the experiment. Experimental protocols were approved by the University of Alberta Health Science Animal Care and Use Committee and the University of Calgary Animal Care Committee.

SKP-SCs in media: Adult male Fischer rats (NHsd; 250–275 g; $N = 31$; Harlan, Indianapolis, IN, USA) were used in this experiment. All procedures were approved by the University of British Columbia Animal Care Committee in accordance with the guidelines of the Canadian Council on Animal Care.

2.2. SKP-SC preparation procedures

SKP-SCs in hydrogel: Following an overdose of sodium pentobarbital (27.3 mg kg^{-1}; IP injection), back skin was shaved, cleaned with 70% EtOH and

then removed from 12 week old male Fischer (CDF®) rats (Charles River). Adult SKPs were isolated as previously described (Biernaskie *et al* 2007a, Hagner and Biernaskie 2013, Kumar *et al* 2016). Briefly, skin was floated on dispase (5 U ml^{-1}; Stem Cell Technologies, Vancouver, BC, Canada) for 2 h at 37 °C. Epidermis was removed and discarded, while the dermis was digested with collagenase Type IV (1 mg ml^{-1}; Worthington, Burlington, ON, Canada) and then subsequently dissociated to single cells by manual trituration. Isolated primary dermal cells were plated at 50 000 cells ml^{-1} in SKP proliferation medium consisting of DMEM and F-12 nutrient supplement at a 3:1 ratio (Invitrogen, Carlsbad, CA, USA) with basic fibroblast growth factor (40 ng ml^{-1}; BD Biosciences, Mississauga, ON, Canada), 2% B27 supplement (Invitrogen) and 1% penicillin/streptomycin (Invitrogen).

Following two serial passages, floating spherical colonies were pelleted by centrifugation and dissociated in collagenase Type IV for 5 min at 37 °C. SKPs were dissociated via gentle trituration, washed twice with sterile HBSS and then plated on plastic culture dishes coated with poly-d-lysine (20 μg ml^{-1}) and laminin (4 μg ml^{-1}; both from BD Biosciences) at 50 000 cells ml^{-1} in SC proliferation medium, DMEM/F-12 (3:1; Invitrogen) containing 1% N2 supplement (Invitrogen), 1% penicillin/streptomycin (Invitrogen), neuregulin (50 ng ml^{-1}; R&D Systems, Minneapolis, MN, USA), and forskolin (5 μM; Sigma-Aldrich Canada Ltd, Oakville, ON, Canada). SC differentiation was verified by their adoption of a bipolar morphology (supplementary figure 1 is available online at stacks.iop.org/BMM/13/034101/mmedia), formation of adherent parallel cellular arrays and their expression of the p75NTR (see below), all well characterized features of rodent SCs (Morrissey *et al* 1991, Vroemen and Weidner 2003).

To enable long term tracking, SKP-SCs were labeled using a replication deficient lentiviral vector encoding green fluorescent protein (GFP) as described previously (Rahmani *et al* 2014, Kumar *et al* 2016). SKP-SCs were allowed to reach 40% confluence and then grown in supernatant containing lentiviral particles in the presence of polybrene (8 μg ml^{-1}; Sigma-Aldrich Canada Ltd) for 18 h. Subsequently, SKP-SCs were washed twice with DMEM, the media replaced, and further expanded for 5–10 passages prior to FACS selection of p75^{+}/GFP^{+} cells.

To purify GFP^{+} cells, SKP-SCS were grown to 60% confluence, trypsinized (trypsin-EDTA 0.25%; Thermo Fisher, Waltham, MA, USA) for 3 min, gently triturated and suspended in HBSS containing 10% FBS to quench the trypsin. SKP-SCs were resuspended in HBSS containing 1% bovine serum albumin and p75^{+}/GFP^{+} cells were selectively isolated using a FACS Aria III cell sorting system (BD Biosciences). FACS data analysis parameters (i.e., gates) were based on control cultures of GFP^{-} rat SKP-SCs and positive

controls consisting of SKP-SCs isolated from GFP-expressing transgenic rats (Sparling *et al* 2015).

SKP-SCs in media: To start a culture of SKPs, a group of rats ($n = 5$) were euthanized upon arrival to the animal facility. Briefly, the back of the rats was shaved and back skin samples were collected and placed in 50 ml falcon tubes in DMEM with low glucose, placed on ice, and shipped to the University of Calgary, where SKPs were isolated, differentiated into SCs and labeled with GFP. SKP-SCs were isolated from the same batch of rats into which the cells were transplanted to avoid the need for immunosuppression. Cell culturing and transduction methods were as described for the SKP-SCs in hydrogel study.

2.3. Mycoplasma polymerase chain reaction (PCR)
PCR was performed only for the SKP-SCs in hydrogel study. PCR was conducted for the presence of mycoplasma, since this has been previously demonstrated to accelerate transformation of other cell types (Tsai *et al* 1995, Feng *et al* 1999). Frozen stock of GFP$^+$ SKP-SC lines 1 and 3 were thawed and cultured for 7 days in the absence of antibiotics. In addition, 25 μm horizontal spinal cord sections from a graft recipient rat were scraped off from slides post-processing and tested. Supernatant was removed, boiled for 10 min and then diluted in molecular grade water. PCR was performed using iProof HF MasterMix (Bio-Rad Laboratories, Inc., Hercules, CA, USA) amplification in accordance with previously published protocol (Choppa *et al* 1998). Primers were as follows: 5' GGG AGC AAA CAG GAT TAG ATA CCC T 3' and 5' TGC ACC ATC TGT CAC TCT GTT AAC CTC 3'. PCR reactions were performed as follows: 98 °C, 3 min; followed by 39 cycles of 98 °C for 10 s; 55 °C, 30 s (annealing); and then 72 °C for 5 min.

2.4. HAMC and eHAMC preparation
HAMC vehicles for SKP-SC transplantation were only used in the SKP-SCs in hydrogel study. MC (Mw 310 kDa, Shin-Etsu Metolose SM- 4000, Japan) conjugated with the cell adhesive peptides RGD or IKVAV was prepared as previously described (Tam *et al* 2012). Briefly, MC was thiolated first, the reactive thiol was then reacted with maleimide-peptide by Michael-type addition. Maleimide-peptides were synthesized using an automated peptide synthesizer. Since it has been demonstrated that longer peptide sequences have greater biological activity/binding capacity than shorter sequences (Craig *et al* 1995), we used the peptide sequences Ac-GRGDS-PASSK-G$_4$-SR-L$_6$-R$_2$KK(Maleimide)G, where RGD is the fibronectin-derived adhesion sequence, and (Maleimide)-GRKQAAS-IKVAV-SG$_4$SRL$_6$R$_2$KK(Alloc)-G, were IKVAV is the laminin-derived adhesion sequence. The peptides were conjugated to different polysaccharide chains. RGD and IKVAV sequences were added, given that these

sequences both promote SC adhesion (Zheng *et al* 2015, Kontoveros 2015).

HAMC and eHAMC hydrogels were prepared as previously described (Führmann *et al* 2016). Briefly, HA (MW 1500 kDa, Dramen, Norway) and MC or MC-RGD/-IKVAV were sterile filtered, lyophilized and stored at 20 °C under sterile conditions. Sterile water was added to HA and MC, MC-RGD/-IKVAV (1% w/v) under aseptic conditions and gently agitated overnight at 4 °C. The dissolved hydrogel was mixed in a speedmixer for 20 s at 3500 rpm, followed by centrifugation at 14 400 RPM for 45 s and cooled on ice until cell addition. As MC forms a loosely cross-linked network through hydrophobic interactions, no crosslinker was added.
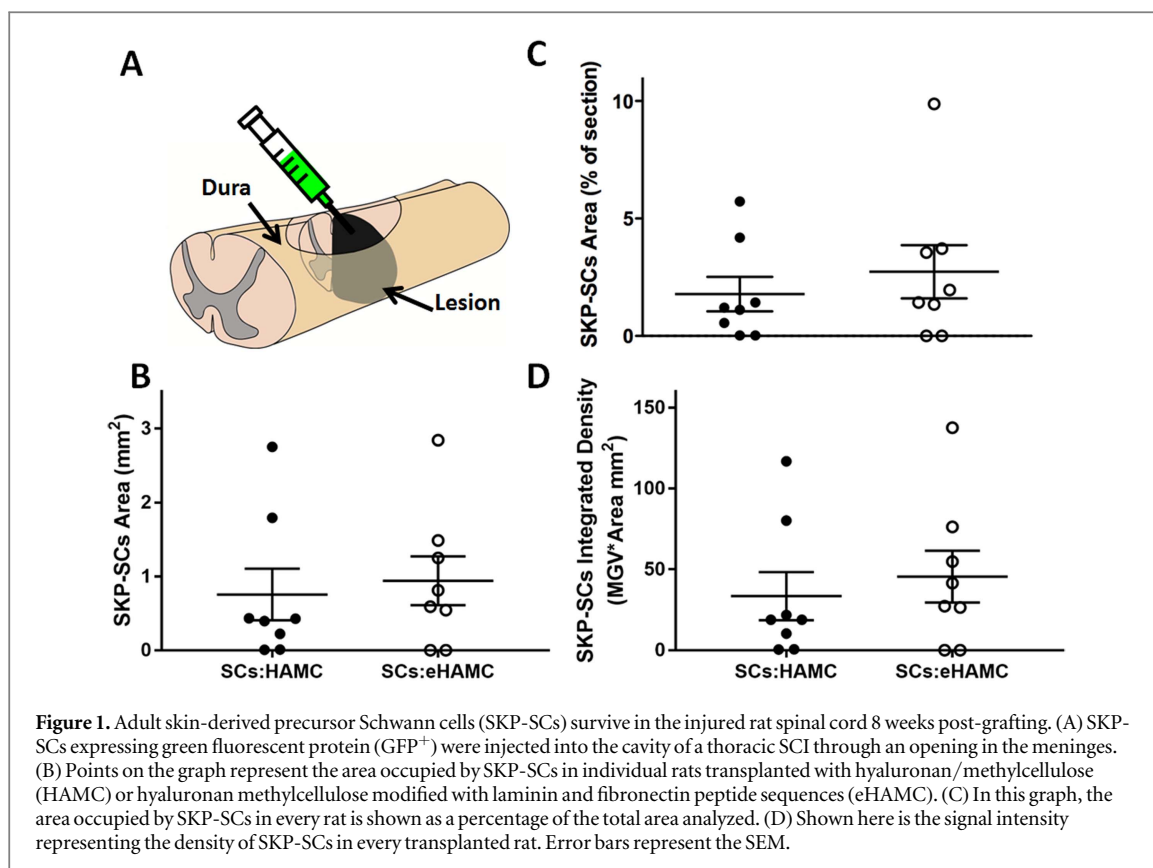
2.5. SKP-SC thawing, plating, and maintenance conditions
SKP-SCs in hydrogel study: Frozen vials of three independent adult lines of GFP$^+$ SKP-SCs were thawed at 37 °C in under 2 min. Thawed suspensions were diluted in DMEM and centrifuged at 1000 rpm for 5 min. The resultant cell pellets were re-suspended at a density of 50 000 cells ml^{-1} in SC proliferation medium. 5% heat inactivated fetal bovine serum (FBS; Invitrogen) was added initially to promote cells' adherence. SKP-SCs were plated on polystyrene 25 cm^2 flasks or 10 cm dishes coated with laminin (4 μg ml^{-1}) and poly-d-lysine (20 μg ml^{-1}; all from Fisher Scientific, Ottawa, ON, Canada). Cells were cultured in an incubator at 37 °C in an atmosphere containing 5% CO$_2$ (Thermo Scientific) and fed every 3 days. SKP-SCs on passage 5–10 were transplanted when the cultures were 75% confluent.

SKP-SCs in media study: Cell culture conditions were as described for the SKP-SCs in hydrogel study with the exception that five independent adult GFP$^+$ SKP-SC lines were used. The cell lines came from 5 rats from the same batch of animals used in the experiment.

2.6. Surgical procedures
SKP-SCs in hydrogel: All surgical procedures were conducted under isoflurane inhalation anesthesia (5% for induction; 2.5%–3.0% for maintenance) supplied with 50:50 air mixed with pure oxygen. The rats' backs were shaved and the skin was disinfected with chlorhexidine digluconate (Sigma-Aldrich Canada Ltd). The lubricant Tears Naturale (Alcon Canada, Inc., Mississauga, ON, Canada) was applied to the eyes to protect them from drying. The skin overlaying the thoracic vertebrae was cut, and the muscles were dissected apart to expose the T8 vertebra, which was removed surgically. Following a horizontal incision of the dura mater along the midline, the right side of the spinal cord was cut with spring scissors. To ensure completeness of the hemisection injury, the lesion site was crushed with Dumont #5 forceps. One percent

Figure 1. Adult skin-derived precursor Schwann cells (SKP-SCs) survive in the injured rat spinal cord 8 weeks post-grafting. (A) SKP-SCs expressing green fluorescent protein (GFP$^+$) were injected into the cavity of a thoracic SCI through an opening in the meninges. (B) Points on the graph represent the area occupied by SKP-SCs in individual rats transplanted with hyaluronan/methylcellulose (HAMC) or hyaluronan methylcellulose modified with laminin and fibronectin peptide sequences (eHAMC). (C) In this graph, the area occupied by SKP-SCs in every rat is shown as a percentage of the total area analyzed. (D) Shown here is the signal intensity representing the density of SKP-SCs in every transplanted rat. Error bars represent the SEM.

dry agarose film was placed on top of the incision in the dura mater. The purpose of the agarose film was to cover the incision in the dura and prevent scarring. This also greatly facilitated the resection for cell implantation. Muscles were sutured with vicryl 5-0 (Johnson & Johnson Medical Pty Ltd, Sydney, NSW, Australia), and the skin was stapled with 9 mm stainless steel clips (Stoelting Co., Wood Dale, IL, USA). Animals received 0.04 mg kg^{-1} buprenorphine SQ (Temgesic, Schering-Plough, Kirkland, QC, Canada) at the start of the operation, followed by a 0.02 mg kg^{-1} dose 8 h afterwards. Animals were kept hydrated with a 4 ml saline SQ injection immediately post-operatively and a 2 ml dose the day after surgery. Bladders were manually expressed until voiding was re-established. One rat was euthanized with a pento-barbital overdose (Euthanyl; Biomeda-MTC, Cam-bridge, ON, Canada) at 1000 mg kg^{-1} IP due to its lack of recovery.

Two weeks post-SCI, rats received either no treat-ment (the spinal cord was re-exposed and a Hamilton needle tip was inserted into the lesion cavity, $n = 6$) or were given one of three different treatments: 0.5%/0.5% eHAMC injection alone ($n = 7$), SKP-SCs in 0.5%/0.5% HAMC ($n = 8$), or SKP-SCs in 0.5%/0.5% eHAMC ($n = 8$). Immediately before transplanta-tion, SKP-SCs were detached from dishes using Tri-ple E express (Invitrogen) and gently pipetted to create a cell suspension. The suspension was centrifuged at 1000 rpm for 5 min and the pellet re-suspended in DMEM. The cell suspension was mixed with HAMC or eHAMC for a final 0.5%/0.5% dilution (∼50 000 cells μl^{-1}). A total volume of 4 μl (∼200 000 total cells) was injected into the epicenter of the lesion using a 10 μl Hamilton syringe (figure 1(A)). The injection site was covered with agarose film. Agarose film was used to cover the injection site to prevent backflow of transplanted cells. Buprenorphine was administered (0.03 mg kg^{-1}) pre-operationally and 2.5 ml of saline was given right after the surgery and the following morning. All of the animals received daily cyclosporine A injections (15 mg kg^{-1}, SQ; Novartis, Dorval, QC, Canada) starting 1 day before transplantation and continuing until euthanasia.

SKP-SCs in media: Rats ($n = 26$) underwent a unilateral C5 laminectomy followed by a hemi-contu-sion SCI on the left or right side of the spinal cord. The side of the hemi-contusion was based on paw pre-ference as determined with the single pellet-grasping task developed by Whishaw *et al* (1998). Contusions were carried out using the IH impactor with a force of 150 kdynes using a custom clamping system as pre-viously described (Lee *et al* 2012) and animal care was similar to that described for the SKP-SCs in hydrogel study. Rats received cell (SKP-SC group $n = 13$) or media injections (injury only control group $n = 13$) 2 weeks post-SCI. GFP$^+$ SKP-SCs were re-suspended in DMEM and a Hamilton microsyringe was used to inject 1 μl of cell suspension (∼200 000 cells) into the lesion cavity.

2.7. Behavioral assessment

SKP-SCs in hydrogel: Hindlimb locomotor recovery was assessed on a weekly basis from 1 week post-SCI to 8 weeks after injury (6 weeks post-grafting) using the Basso, Bresnahan and Beattie (BBB) locomotor rating scale (Basso *et al* 1995) by two blinded observers 2 min after voiding the bladder, as spontaneous micturition may elicit reflex hindlimb activity (Thor *et al* 1983, Tai *et al* 2006).

SKP-SCs in media: One week following transplantation, SKP-SC rats demonstrated a health decline and deterioration of forelimb function. The termination point was defined as loss of 15% of the original body weight, porphyrin staining around the eyes, and paralysis of the upper limbs.

2.8. Perfusion and histology

SKP-SCs in hydrogel: All rats were euthanized 10 weeks post-SCI (8 weeks post-grafting) with a lethal dose of pentobarbital and transcardially perfused with saline containing heparin followed by phosphate-buffered 4% paraformaldehyde with 5% sucrose (PFA; 0.1 M; pH 7.4). Spinal cords were removed, post-fixed in 4% PFA overnight at 4 °C, and cryoprotected in 30% sucrose for 5 days. Thoracic spinal cord blocks with the lesion in the center were embedded in O.C.T (Sakura Finetek, Torrance, CA, USA), mounted onto filter paper, and frozen in dry ice cooled 2-methylbutane (Fisher Scientific). Sections of the spinal blocks were cut horizontally at a thickness of 25 μm on a NX70 cryostat (Fisher Scientific), staggered across four sets of slides (Fisher Scientific, Ottawa, ON, Canada) and stored in a −20 °C freezer until further processing.

For immunohistochemistry, spinal cord sections were permeabilized and non-specific IgG binding blocked with 10% normal goat serum (NGS) in 0.5% Triton X-100 (TBS-TX) for 1 h. Primary antibodies in 1% NGS in TBS were applied to slides overnight at 4 °C. Then, slides were incubated with fluorophore-conjugated secondary antibodies for 2 h at room temperature, dehydrated with increasing ethanol concentrations (50%, 75%, and twice with 99% for 2 min each) and mounted with cytoseal or coverslipped without dehydration with Fluoromount G (Southern Biotech, Birmingham, AL, USA). The primary antibodies used were: polyclonal chicken anti-GFP (1:1000; Abcam, Toronto, ON, Canada), monoclonal (clone GA5) mouse anti-glial fibrillary acidic protein (GFAP; 1:700; Chemicon, Temecula, CA, USA), polyclonal rabbit anti-S100 (1:1000; Abcam), monoclonal (clone 192) mouse anti-p75 (1:500; Advanced Targeting Systems, SD, CA, USA), monoclonal (clone 2Q178) mouse anti-nestin (1:1000; Abcam), polyclonal rabbit anti-fibronectin (1:100; Chemicon), and polyclonal rabbit anti-ki-67 (1:100; Abcam).

Secondary antibodies used were Alexa Fluor 488 goat anti-chicken, Alexa Fluor 555 goat anti-mouse, Alexa Fluor 555 goat anti-rabbit, Alexa Fluor 647 goat anti-mouse, and Alexa Fluor 647 goat anti-rabbit (1:500; all from Invitrogen).

Immunofluorescence imaging was carried out with an automated upright Leica DM6000 B microscope system (Leica Microsystems Inc., Richmond Hill, ON, Canada).

For H&E staining, horizontal sections of spinal cord were stained with hematoxylin and eosin. Slides were hydrated and stained with Ehrlich's hematoxylin for 10 min, followed by differentiation in 1% acid alcohol solution for 10 s. Sections were 'blued-up' with ammonia water solution (0.2% ammonium hydroxide in distilled water) for 1 min, stained with eosin for a few sec, dehydrated, cleared in two 5 min baths of xylene, and mounted with Permount^R. Staining was visualized with a Leica DMLB microscope (Leica Microsystems Inc.).

SKP-SCs in media: Rats were perfused 1–4 weeks post-transplantation when they reached a pre-determined experimental termination point (loss of 15% of original body weight, porphyrin staining around the eyes, and paralysis of the upper limbs). All injury only rats were perfused 4 weeks post-media injections. Animals received a lethal dose of chloral hydrate (100 mg kg^{-1}, IP; BDH VWR Analytical, Radnor, PA, USA) and were transcardially perfused with PBS followed by 4% PFA. The cords were post-fixed in 4% PFA overnight, cryoprotected in graded sucrose solutions and frozen in O.C.T (Fisher Scientific). The injured tissue was sectioned in 20 μm cross-sections.

Tissue from a subset of rats (SKP-SCs $n = 5$; injury only $n = 6$) underwent immunohistochemistry to identify the status of the lesion site at 4–5 weeks post-injury (2–3 weeks post-transplantation). For immunohistochemistry, frozen sections were thawed, rehydrated and incubated in 10% normal donkey serum for 30 min and primary antibodies were applied overnight. After washes, secondary antibodies were applied for 2 h, and slides were washed and coverslipped. The following primary antibodies were used: mouse anti-neurofilament 200 (NF-200; 1:500; Sigma-Aldrich Canada Ltd); mouse anti-β-3-tubulin (βIII-tubulin; 1:500; Sigma-Aldrich Canada Ltd), goat anti-GFP (1:200; Rockland Immunochemicals, Gilbertsville, PA, USA), and rabbit anti-GFAP (1:1000; Dako Canada ULC, Mississauga, ON, Canada). Axons were stained using a combination of NF-200 and βIII-tubulin. The secondary antibodies were generated in donkey and directed to the host of the primary antibody and conjugated with Alexa Fluor fluorochromes 405, 488, and 594 at a concentration of 1:200 (Jackson ImmunoResearch Laboratories, West Grove, PA, USA). Immunofluorescence was captured using a Zeiss AxioObserver Z1 inverted confocal microscope fitted with Yokogawa spinning disk and Zen 2012 software (Zeiss, North York, ON, Canada).

2.9. Anatomical analysis

The anatomical analyses described below were only conducted for the SKP-SCs in hydrogel study, since the SKP-SCs in media study was terminated early due to health complications of animals receiving grafts.

Cell survival: All analyses were carried out using ImageJ 1.43 μ (National Institutes of Health, Bethesda, MD, USA), on five horizontal spinal cord sections 275 μm apart encompassing the lesion epicenter. The perimeter of each horizontal section was drawn and the GFP$^+$ region within the perimeter was thresholded. The entire horizontal section area in mm^2, area of the GFP$^+$ region in mm^2, and GFP$^+$ signal intensity (integrated density: mean gray value of pixels (MGV)*the area analyzed in mm^2) were measured and averaged across the five sections. The area of GFP$^+$ cells was calculated alone or as a percentage of the area of the horizontal section analyzed.

To estimate the number of surviving SKP-SCs, a z-stack in the center of a graft was captured at 630× with a Leica DMi8 confocal microscope (Leica Microsystems Inc.). Z step size was 0.5 μm. The number of GFP$^+$ cell bodies in the z-stack was counted using the cell counter plug-in on ImageJ 1.43 μ. The 'show all' option was selected, so that all cells counted were labeled and cells were not counted twice. Next, the steps of the z-stack were summed and the resulting image was thresholded to identify the area (mm^2) of GFP$^+$ cells. The number GFP$^+$ cells was, then, divided by the GFP$^+$ area to determine the concentration of GFP$^+$ cells per unit area. The number of GFP$^+$ cells per section was calculated by multiplying the GFP$^+$ area of each section by the concentration of GFP$^+$ cells per unit area

To estimate the number of GFP$^+$ cells in between sections, the average GFP$^+$ area of two adjacent sections was taken, multiplied by the concentration of GFP$^+$ cells per unit area, and multiplied by the number of sections in-between adjacent sections on a slide (11 sections).

Lastly, the total number of GFP$^+$ cells in the spinal cord of each animal was calculated by summing the number of SKP-SCs found in each section and the number of SKP-SCs in between sections.

Cell spreading: The rostral and caudal spread of the GFP$^+$ cells from the lesion epicenter, which was identified by an inward deformation of the parenchyma, was measured in mm using ImageJ 1.43 μ. Results from five sections 275 μm apart imaged at 50x were averaged. Cell spreading measurements included GFP$^+$ cells located within the spinal parenchyma and along the perimeter of the spinal cord. We also measured spreading of GFP$^+$ cells in the parenchyma alone, because we made the observation that thin trails of cells spread along the perimeter but large clusters of cells formed in the parenchyma, causing tissue displacement and destruction.

Cross-sectional lesion size: Every horizontal spinal cord section comprising the SCI from one set of slides was imaged under phase-contrast microscopy. The lesion was identified by the disruption of typically linear organization of white matter tracts on the outside of the spinal cord and the loss of darkly appearing cell bodies of the gray matter located centrally. Maximum lesions were re-constructed by hand on a T9 (overlayed by vertebra T8) cross-section schematic obtained from the Atlas of the Rat Spinal Cord (Watson *et al* 2009). The area of the lesioned tissue was then calculated as a percentage of the T9 cross-sectional area.

Lesion length: Horizontal spinal cord sections comprising the SCI were stained for GFAP to show the lesion borders. Overview images of the sections at 50× magnification were analyzed on ImageJ 1.43 μ. The distance in μm between the rostral and caudal lesion borders (i.e., the length of the lesion) was measured and averaged across five sections 275 μm apart.

White matter compression: Given the finding that grafted GFP$^+$ SKP-SCs appeared to form growths in the spinal cord, we evaluated if the growths were compressing surrounding spared white matter. One section encompassing the injury epicenter and stained for GFP and GFAP was analyzed. The thickness of the white matter in the hemicord opposite the transplant was measured in μm. The thickness of the white matter was also measured below the transplant. Only rats that were considered to have formed growths were included in this analysis (SCs:HAMC $n = 5$; SCs: eHAMC $n = 6$). Clusters of GFP$^+$ cells were considered growths if the clusters contained more than 2x the original number of transplanted GFP$^+$ cells, showed features of SC tumors (i.e., Schwannomas), and were positive for the proliferation marker ki-67. White matter thickness of lesion only rats ($n = 6$) ~2000 μm above and below the SCI was measured as a control.

Transplant morphological assessment: Analysis of the transplant for features of Schwannomas was developed based on writings from *Nervous System: Cambridge Illustrated Surgical Pathology* by Hannes (2009). Every other horizontal spinal cord section containing the transplant and stained with H&E was assessed under bright-field microscopy at 50× magnification. The presence of dense Antoni A cellular patterns with palisading nuclei surrounding pink regions (Verocay bodies), relatively sparse Antoni B areas (Wippold *et al* 2007), and signs of hemorrhage, such as red pigmentation (Hatae *et al* 2014), were recorded. The size and shape of the cells were evaluated under 100× magnification.

2.10. Statistical analysis

Statistical analysis was only conducted for the SKP-SCs in hydrogel study, as only this study collected

quantitative data. All results were analyzed with GraphPad Prism 7 (GraphPad Software Inc., La Jolla, CA, USA). D'Agostino-Pearson omnibus test was used to assess normality. When data were normally distributed, paired and unpaired two-tailed t-tests were used to make between-group comparisons. Non-parametric alternatives used for unpaired and paired t-tests were Mann–Whitney U and Wilcoxon-matched pairs signed rank tests respectively. Kruskal–Wallis followed by Dunn's tests were used for comparing multiple groups. Cross-sectional lesion size and lesion length were first assessed with Kruskal–Wallis and, then, select pairs of data sets were compared with unpaired t-tests or Mann–Whitney U tests. Repeated measures two-way ANOVA followed by Bonferroni's post-test were used to compare weekly locomotor scores. Scores 1 week post-SCI (before transplants) were also analyzed to ensure all groups had similar motor deficits. Data are presented as mean values $\pm$ SEM, and the threshold for significance was set at a p-value of <0.05.

3. Results

3.1. SKP-SCs in hydrogel study

3.1.1. SKP-SC survival post-transplantation
To measure survival of grafted cells, the GFP$^+$ area in the spinal cord was compared between animals that received GFP$^+$ SKP-SCs in either HAMC or eHAMC. The area covered by SKP-SCs was not significantly different ($p = 0.71$) between the HAMC (0.76 ± 0.35 mm^2) and eHAMC (0.94 ± 0.33 mm^2) groups (figure 1(B)). The area populated by GFP$^+$ cells as a percentage of the horizontal section area also did not differ statistically ($p = 0.72$) between HAMC ($1.8 \pm 0.73\%$) and eHAMC ($2.7 \pm 1.1\%$) groups (figure 1(C)). The third measure of cell survival integrated density (see methods) did not show statistical differences ($p = 0.59$; HAMC 34 ± 15 MGV*mm^2; eHAMC 46 ± 16 MGV*m^2; figure 1(D)). Finally, the estimated number of GFP$^+$ cells was not statistically different ($p = 0.62$; HAMC $1\,195\,774 \pm 565\,604$ GFP$^+$ cells; eHAMC $1\,596\,055 \pm 557\,613$ GFP$^+$ cells). This means that ~6× the number of originally grafted cells (~200 000) were found in the spinal cord of HAMC animals and ~8× the number of originally grafted cells were found in the spinal cord of eHAMC animals. These estimates suggest GFP$^+$ SKP-SCs proliferated post-grafting. It should be noted, two rats from the HAMC group and two rats from the eHAMC group exhibited <10% survival of originally grafted cells. Thus, the rats with low survival were excluded from analysis of cell spreading. Low survival of grafted cells in a few rats may have resulted from increased severity of the original injury. The majority of cells identified by thresholding were located up to 15 mm beyond the injury/transplantation site.
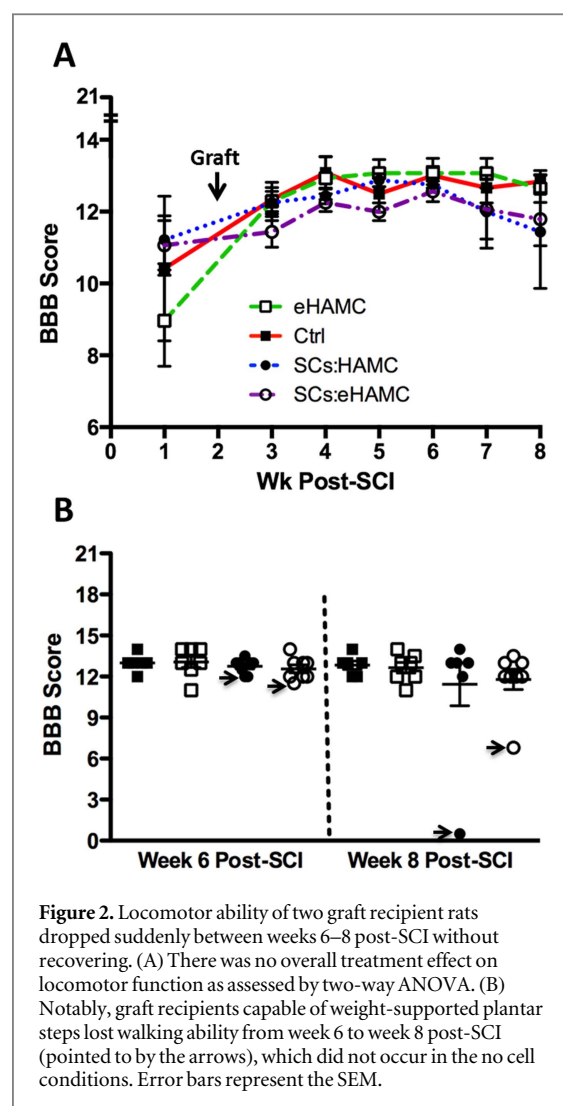

Figure 2. Locomotor ability of two graft recipient rats dropped suddenly between weeks 6–8 post-SCI without recovering. (A) There was no overall treatment effect on locomotor function as assessed by two-way ANOVA. (B) Notably, graft recipients capable of weight-supported plantar steps lost walking ability from week 6 to week 8 post-SCI (pointed to by the arrows), which did not occur in the no cell conditions. Error bars represent the SEM.

3.1.2. Open-field locomotion
The BBB locomotor rating scale was used to determine the influence of SKP-SC transplantation and hydrogel formulation on functional recovery. Locomotor scores were comparable between groups 1 week after hemisection SCI ($p = 0.64$). As to be expected following a hemisection, open-field scores were significantly improved from week 1 to week 8 post-SCI ($p < 0.0001^{****}$); however, there was no significant difference between the treatment groups in terms of BBB scores at any time point ($p = 0.75$; figure 2(A)). Average BBB scores were not significantly different from week 6 to week 8 post-SCI: 13 ± 0.26 to 12.8 ± 0.31; 13.1 ± 0.41 to 12.6 ± 0.39; 12.8 ± 0.19 to 11.4 ± 1.57; and 12.6 ± 0.29 to 11.8 ± 0.74 for the lesion only control, eHAMC, SCs:HAMC, and SCs:eHAMC groups respectively. While the group averages were not significantly different, we noted that between 6 and 8 weeks post-SCI one animal in the SCs:HAMC (score 12 to 0.5) and one in the SCs:eHAMC (score 11.5 to 6.8) groups lost weight-supported hindlimb stepping (figure 2(B)). A BBB score of at least 10 represents weight-supported plantar stepping.
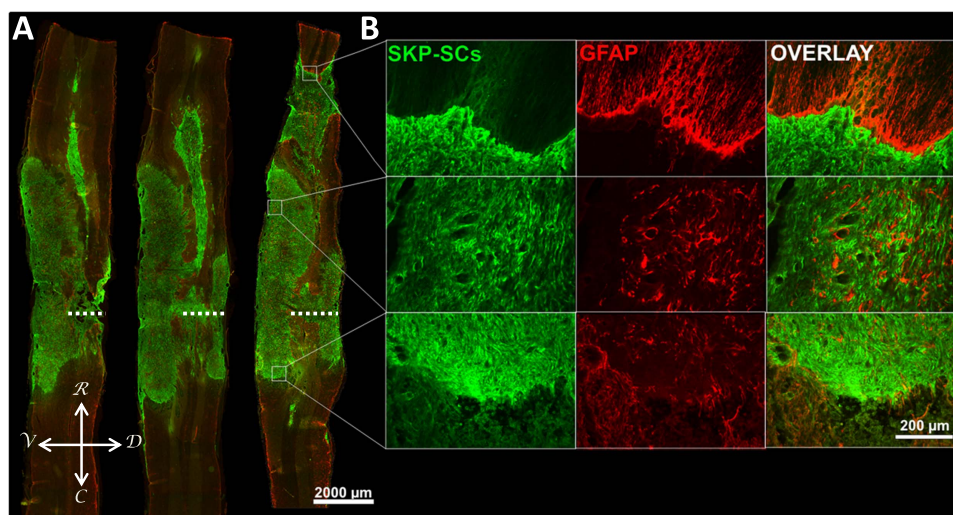
Figure 3. Adult SKP-SCs spread extensively in the spinal cord and are sharply bordered by reactive astrocytes. (A) Horizontal sections of spinal cord immunolabeled for GFP, expressed by transplanted SKP-SCs (green). Sections were also stained for the reactive astrocyte marker GFAP (red). Although SKP-SCs were injected into the lesion cavity, the cells were found throughout most of the dorso-ventral and rostro-caudal axes of the spinal block analyzed. R = rostral. C = caudal. V = ventral. D = dorsal. (B) Magnification images of insets reveal intense GFAP signal along the graft borders. Data shown belongs to the SCs:HAMC subject whose walking deteriorated. The dotted white line denotes the hemisection level.
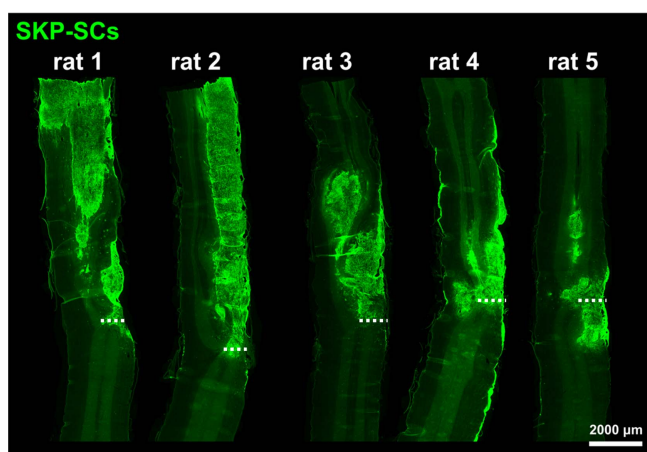

Figure 4. Extent of adult SKP-SC spread varies between graft recipient rats. Shown here are horizontal spinal cord sections near the central canal of five different animals. The SKP-SCs spread in all cases but cell distribution and magnitude of spread were dissimilar. Rat 1 is the SCs:eHAMC subject whose function worsened. Rats 2–5 did not exhibit a functional decline. The dotted white line denotes the hemisection level.
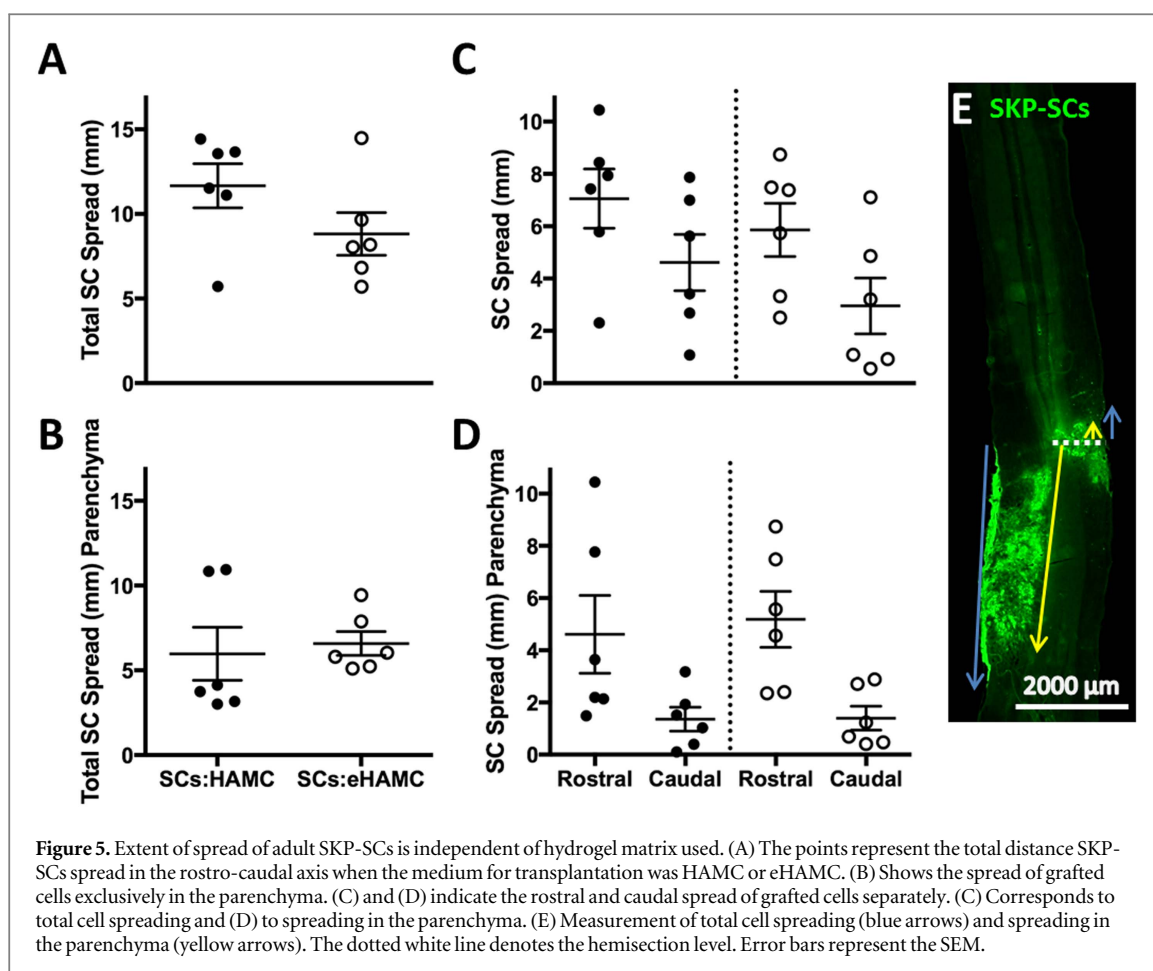
Weight-supported stepping of rats that did not receive cells was unaffected.

3.1.3. Analysis of SKP-SC spreading post-transplantation
Grafted GFP$^+$ SKP-SCs spread to undamaged spinal cord tissue near the site of injury in every subject with clear borders between the graft and host tissue. This is shown by the distinct separation between reactive astrocytes and grafted cells, irrespective of where grafted cells were found in the spinal cord (figure 3). Spreading of grafted cells to the perimeter of the spinal cord was seen in all animals. Large masses/growths of GFP$^+$ cells were found in areas of originally uninjured parenchyma in 5 out of $n = 8$ HAMC and 6 out of $n = 8$ eHAMC rats (figure 4). Masses of GFP$^+$ cells were considered growths if the masses had more than $2\times$ the original number of grafted cells, morphological features of Schwannomas, and ki-67 positivity.

To further characterize the spreading of grafted GFP$^+$ SKP-SCs, we measured the distance covered by the cells. Distance spread in both parenchyma and along the perimeter did not differ between the SCs:HAMC or SCs:eHAMC groups (figure 5(A); $p = 0.24$). The mean total distance in mm covered by SCs:HAMC and SCs:eHAMC cells was 12 ± 1.3 mm and 8.8 ± 1.3 mm respectively. The distance GFP$^+$ SKP-SCs spread exclusively in the parenchyma was comparable between the SCs:HAMC and SCs:

Figure 5. Extent of spread of adult SKP-SCs is independent of hydrogel matrix used. (A) The points represent the total distance SKP-SCs spread in the rostro-caudal axis when the medium for transplantation was HAMC or eHAMC. (B) Shows the spread of grafted cells exclusively in the parenchyma. (C) and (D) indicate the rostral and caudal spread of grafted cells separately. (C) Corresponds to total cell spreading and (D) to spreading in the parenchyma. (E) Measurement of total cell spreading (blue arrows) and spreading in the parenchyma (yellow arrows). The dotted white line denotes the hemisection level. Error bars represent the SEM.

eHAMC groups (figure 5(B); $p = 0.39$). The distance covered by the cells within the parenchyma alone was 6.0 ± 1.6 mm and 6.6 ± 0.70 mm for the SCs:HAMC and SCs:eHAMC groups respectively.

Grafted cells spread both rostral and caudal to the SCI. No statistically significant difference was found on the direction of spread. When transplanted in HAMC, cells expanded a total distance of 7.1 ± 1.1 mm rostrally and 4.6 ± 1.1 mm caudally ($p = 0.31$). In eHAMC, cells expanded a total distance of 5.9 ± 1.0 mm rostrally and 3.0 ± 1.1 mm caudally ($p = 0.31$; figure 5(C)). Spreading in the parenchyma alone was similar with cells expanding both rostrally and caudally in the HAMC (rostral spread: 4.6 ± 1.5 mm; caudal spread: 1.4 ± 0.5 mm; $p = 0.06$) and eHAMC (rostral spread: 5.2 ± 1.1 mm; caudal spread: 1.4 ± 0.5 mm; $p = 0.16$; figure 5(D)) groups.

3.1.4. Morphological analysis of SKP-SC growths
SKP-SC growths were compared to Schwannomas, tumors consisting of SCs (Wippold *et al* 2007). Comparable to Schwannomas, regions with a high density of cells (Antoni A) were found immediately adjacent to regions with few cells (Antoni B; figure 6(A); Wippold *et al* 2007). Overall, GFP+ SKP-SCs demonstrated a typical SC spindle-like morphology (figures 6(A) and (B)). However, as is seen in Schwannomas, the nuclei

were arranged in horizontal rows, termed palisades, and there was a large degree of pleomorphism (figures 6(A) and (B)). Nuclear palisades are normally separated by anuclear zones, forming a Verocay body. Verocay body anuclear zones were not observed, signaling high mitotic activity (Rodriguez *et al* 2012). Instead, rows of palisading nuclei in Antoni A regions had a marginal space between them (figure 6(C)). There was evidence of bleeding in and around the graft that may have been caused by the growing mass of GFP+ cells compressing the spinal cord and damaging local blood vessels (figures 6(C) and (D)).

3.1.5. SKP-SC characterization post-transplantation
Transplanted GFP+ cells expressed p75 and S100, common SC markers (figures 7(A) and (B)). Many of the GFP+ cells did not stain for either of these markers, raising the possibility that a subset of the SKP-SCs were undifferentiated, proliferating immature SCs. Staining for immature SC proteins nestin and fibronectin showed co-labeling with GFP+ cells (figures 7(C) and (D)), suggesting the SCs lacked a mature phenotype. Ki-67 positive signal confirmed the continued proliferation of GFP+ cells 8 weeks post-grafting, as ki-67 signal overlapped with GFP+ cell bodies (figure 8).
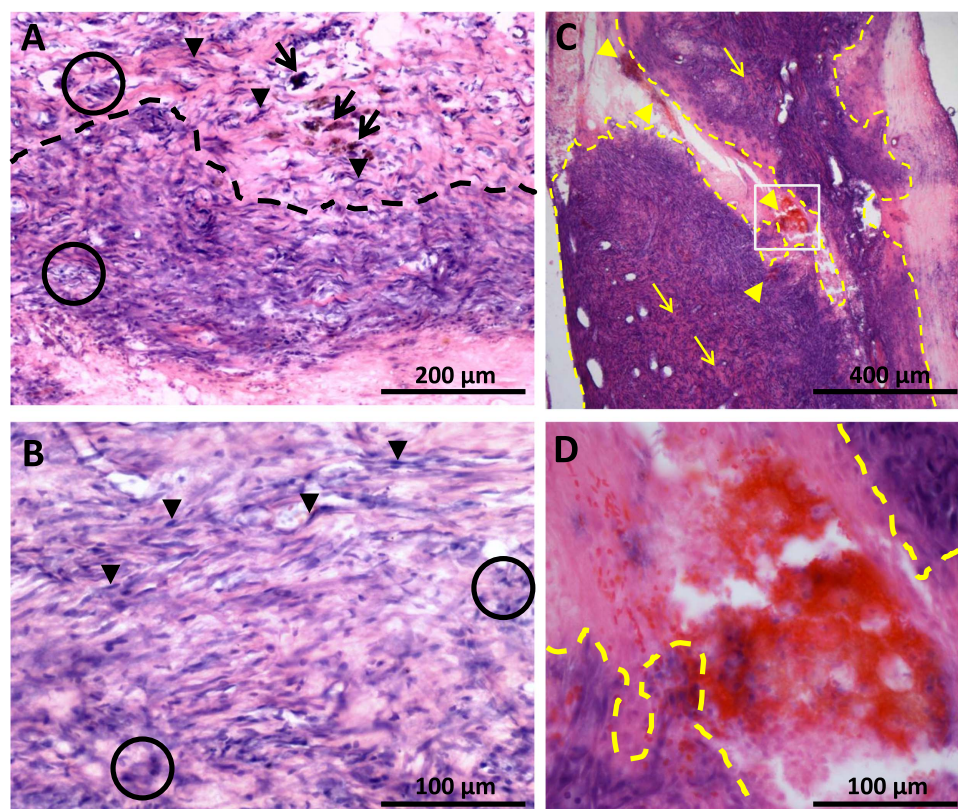
Figure 6. Adult SKP-SC growth exhibits morphological features characteristic of Schwannomas. Pictured here are H&E stained horizontal sections through a SKP-SC growth in the spinal cord. (A) Hyper-cellular Antoni A (below black dashes) and relatively sparse Antoni B regions (above black dashes) are apparent under microscopic examination. (A) and (B) Grafted cells display a spindle shape and nuclei with a slightly undulated contour and tapered or rounded ends (black arrow heads). However, there is some degree of nuclear pleomorphism (circles). Other features include the presence of hemosiderin laden macrophages (black arrows), indicating that the growth underwent hemorrhage. (C) Direct evidence of bleeding within and near the cell graft (yellow arrow heads). (C) There is also an absence of well-formed Verocay bodies due to hyper-cellularity (yellow arrows). The inset in (C) is magnified in (D). (C) and (D) The yellow dashed lines demarcate the graft/spinal cord interface.

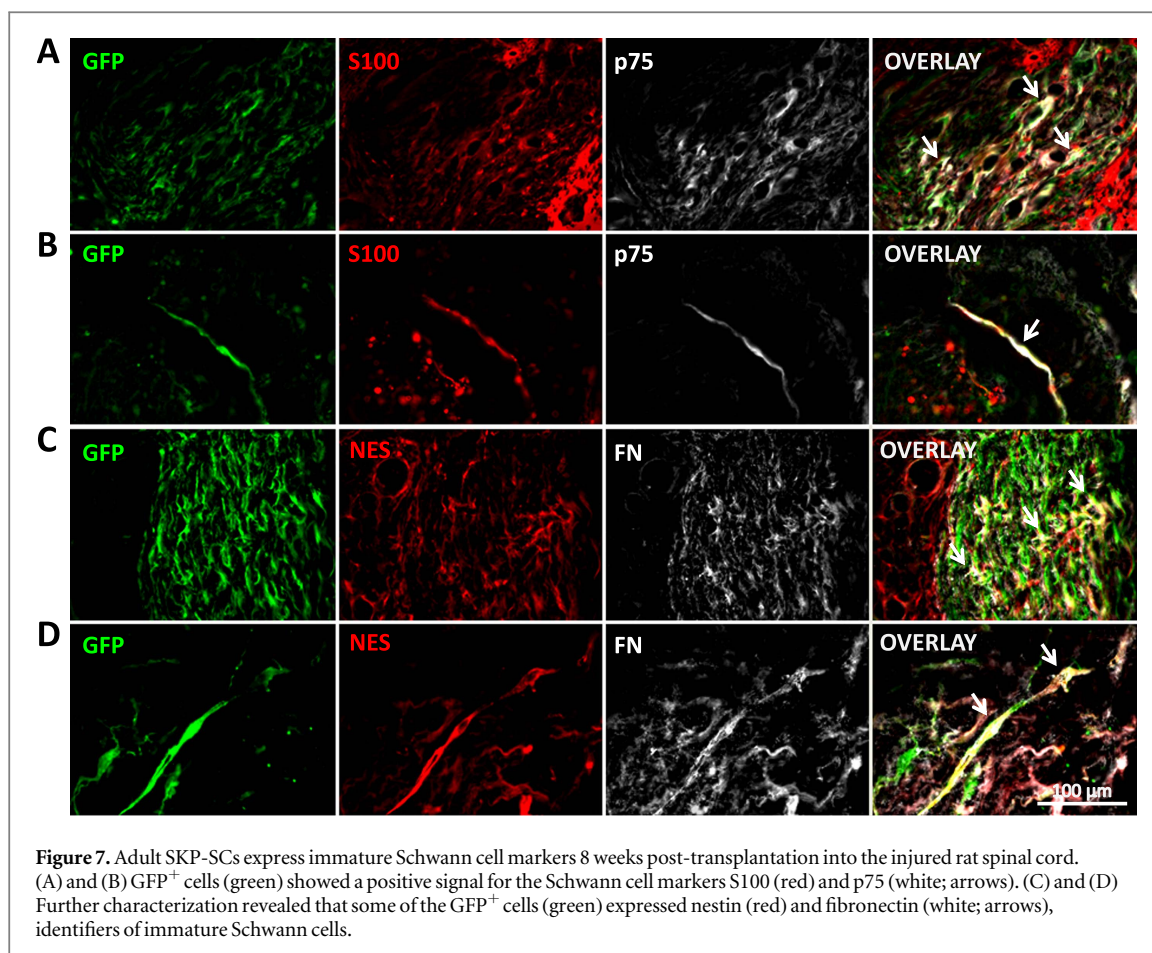*3.1.6. Cross-sectional lesion size and lesion length*

Gray and white matter lesioned tissue was identified on horizontal sections imaged under phase-contrast microscopy and reconstructed on cross-section schematics. Lesioned tissue at the SCI epicenter as a percent of cross-sectional area was significantly different between groups (figure 9; $p < 0.05$). However, Dunn's multiple comparisons test did not identify a difference between group pairs. Group pairs were then compared with Mann–Whitney U, and we found that the SCs:eHAMC group had significantly greater cross-sectional lesions compared to the lesion only and eHAMC groups (both $p < 0.05$). Cross-sectional lesion size was comparable between lesion only versus eHAMC ($p = 0.63$), SCs:eHAMC versus SCs:HAMC ($p = 0.08$), eHAMC versus SCs:HAMC ($p > 0.99$), and lesion only versus SCs:HAMC ($p = 0.85$). Percent cross-sectional lesion size averaged $73 \pm 5.0\%$ for SCs:HAMC, $82 \pm 2.6\%$ for SCs:eHAMC, $71 \pm 4.8\%$ for eHAMC, and $71 \pm 3.7\%$ for the lesion control groups.

The lesion length was analyzed on horizontal spinal cord sections stained for the astrocyte marker GFAP. Statistical analysis with Kruskal–Wallis test did not detect a group effect on lesion length (figure 9; $p = 0.15$), although there was marked variation within the animals that received SKP-SCs, particularly when grafted in combination with eHAMC. Therefore, data pairs were then compared with unpaired t-tests and Mann–Whitney U tests. We found that lesion length was significantly greater between the SCs:eHAMC and lesion only control group ($p < 0.05$). No differences were found between lesion only versus eHAMC ($p = 0.37$), SCs:eHAMC versus eHAMC ($p = 0.05$), SCs:eHAMC versus SCs:HAMC ($p = 0.45$), eHAMC versus SCs:HAMC ($p = 0.54$), and lesion only versus SCs:HAMC ($p = 0.95$) groups. The average spinal cord lesion length of the SCs: HAMC, SCs:eHAMC, eHAMC, and lesion only groups were 2.8 ± 1.1, 3.8 ± 0.90, 1.6 ± 0.17, and 1.5 ± 0.30 mm respectively. The finding that the eHAMC cell transplant group had longer lesions is consistent with the observation that GFP$^+$ signal corresponded perfectly with areas devoid of GFAP labeling.

3.1.7. White matter compression analysis

Host spinal cord tissue appeared distorted where GFP$^+$ cells were abundant. Apparent distortion of host tissue prompted analysis of white matter compression.

Figure 7. Adult SKP-SCs express immature Schwann cell markers 8 weeks post-transplantation into the injured rat spinal cord. (A) and (B) GFP$^+$ cells (green) showed a positive signal for the Schwann cell markers S100 (red) and p75 (white; arrows). (C) and (D) Further characterization revealed that some of the GFP$^+$ cells (green) expressed nestin (red) and fibronectin (white; arrows), identifiers of immature Schwann cells.

White matter thickness on horizontal sections was similar rostral and caudal to the SCI in lesion only control animals ($p = 0.44$). In these rats, the white matter rostral to the lesion was $677 \pm 37\,\mu$m thick and the white matter caudal to the lesion was $792 \pm 51\,\mu$m thick. In SCs:HAMC rats, white matter thickness contralateral to growths and intact tissue was comparable ($p = 0.06$). SCs:HAMC rat white matter contralateral to growths was $585 \pm 107\,\mu$m thick and white matter contralateral to intact tissue was $882 \pm 82\,\mu$m. Contrastingly, SCs:eHAMC rat white matter contralateral to growths was thinner than white matter contralateral to intact tissue ($p < 0.05$; figure 10). SCs:eHAMC white matter contralateral to transplants was $517 \pm 68\,\mu$m thick and white matter contralateral to intact tissue was $811 \pm 44\,\mu$m. In other words, grafted cell growths compressed the white matter of SCs:eHAMC rats only.

3.1.8. SKP-SC testing for mycoplasma
In order to investigate possible reasons for excessive cell division, we examined two SKP-SC cell lines for the presence of mycoplasma, which has been shown to hasten transformation of cells *in vitro* (Tsai *et al* 1995, Feng *et al* 1999). Both of the GFP$^+$ adult SKP-SC lines were found to be positive for mycoplasma, suggesting mycoplasma contamination may have contributed to
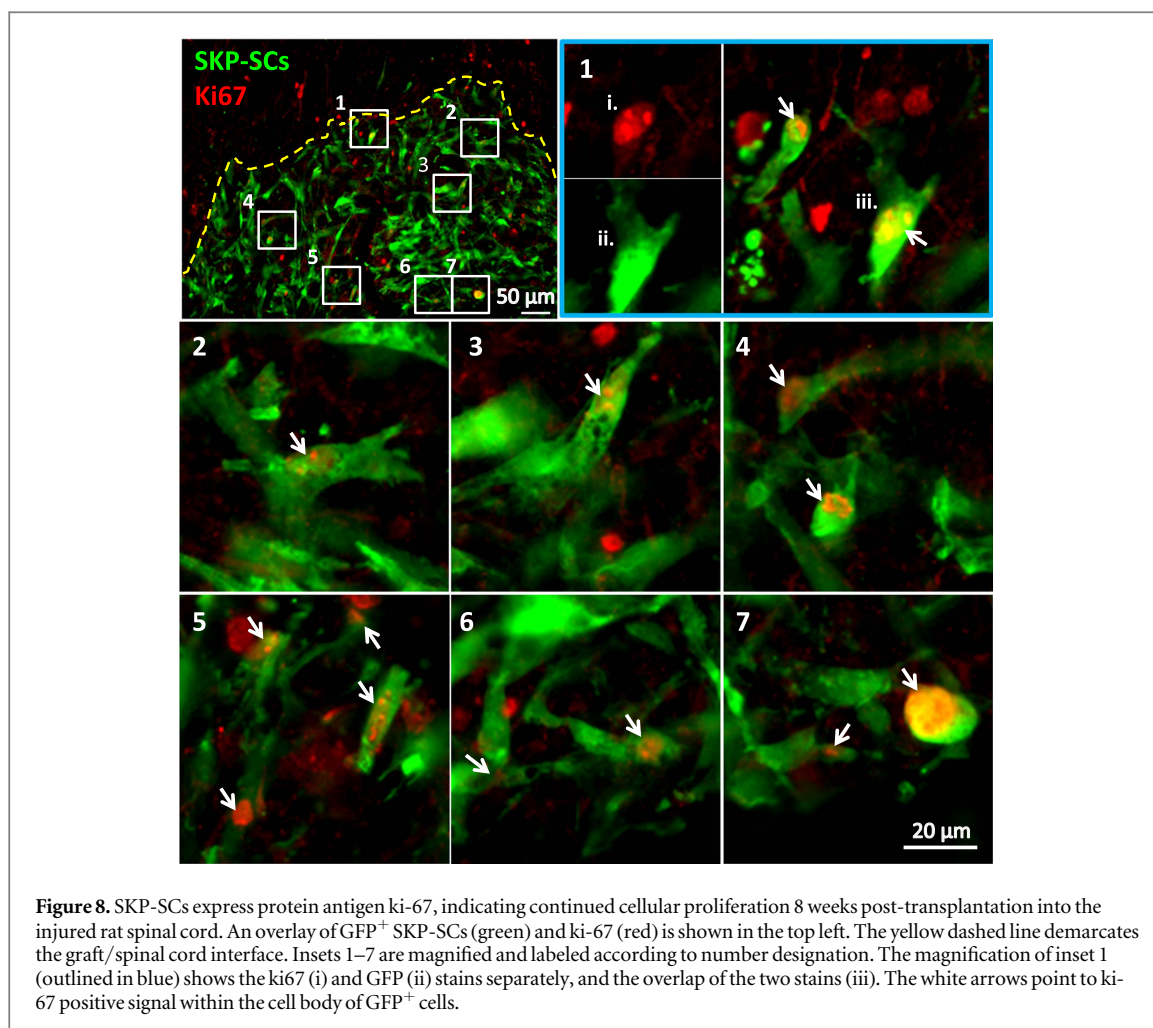
the uncontrolled proliferation of grafted cells (Namiki *et al* 2009).

3.2. SKP-SCs in media study
In an independent experiment, immune competent animals with a contusion SCI had cells transplanted in media or media only injections. The reason for including this study was to show that growth formation can occur with adult SKP-SCs under markedly different conditions.

Many SKP-SC animals demonstrated a behavioral decline 1–4 weeks post-transplantation, reaching pre-determined experiment termination points and as such were euthanized for histological analysis of the injury site. Of the SKP-SC rats: 50% reached the termination point and were perfused before 4 weeks post-transplantation; another 30%–40% demonstrated severe health or behavioral deficits compared to control rats when perfused at 4 weeks post-transplantation; and only 10%–20% appeared in relatively good health at the time of perfusion. In contrast, not a single rat from the injury only control group showed behavioral deterioration or reached the termination point by 4 weeks post-transplantation.

GFP$^+$ growths were found in all the spinal cords of the subset of SKP-SC transplanted rats sectioned for histological analysis. Growths were not found in any of the rats without grafts (figure 11(A)). The growths

Figure 8. SKP-SCs express protein antigen ki-67, indicating continued cellular proliferation 8 weeks post-transplantation into the injured rat spinal cord. An overlay of GFP$^+$ SKP-SCs (green) and ki-67 (red) is shown in the top left. The yellow dashed line demarcates the graft/spinal cord interface. Insets 1–7 are magnified and labeled according to number designation. The magnification of inset 1 (outlined in blue) shows the ki67 (i) and GFP (ii) stains separately, and the overlap of the two stains (iii). The white arrows point to ki-67 positive signal within the cell body of GFP$^+$ cells.

filled the injured cord but also spread to the uninjured cord and resulted in a dramatic decrease in the number of axons at the injury site (figures 11(B) and (C)), likely contributing to the severe behavioral deficits observed.

4. Discussion

To create a bridge for regenerating axons, SCs can be injected into the cavity that forms within the spinal cord after damage (Bunge 1975, Oudega and Xu 2006, Thuret *et al* 2006, Tetzlaff *et al* 2011, Williams *et al* 2015). However, the optimal source of SCs and the approach to ensure maximal graft survival have yet to be determined. SCs may be obtained from peripheral nerves (Murray and Stout 1942) or differentiated from neonatal or adult skin-derived progenitors (Biernaskie *et al* 2007a, Kumar *et al* 2016). Harvesting SKPs is associated with fewer safety concerns and less associated with morbidity than harvesting peripheral nerve SCs (Biernaskie *et al* 2007a). Therefore, SKP-SCs were grafted in the present study. Regardless of source, low survival of SCs post-transplantation is a continuing challenge (Biernaskie *et al* 2007b, Golden *et al* 2007, Pearse *et al* 2007, Enomoto *et al* 2013). Transplanted SC death results from a combination of

factors, including disruption of blood vessels causing ischemic necrosis (Balentine 1978), the inflammatory environment of the injured spinal cord (Hill *et al* 2006), and anoikis (Frisch and Francis 1994, Koda *et al* 2008). The goal of our study was to maximize SKP-SC survival and, hence, cavity filling in the injured rat spinal cord.

To resolve the contribution of inflammation and anoikis on grafted cell loss, we transplanted SKP-SCs in HAMC containing hydrogels. HAMC hydrogel is injectable through a fine gauge needle, biocompatible and biodegradable (Caicco *et al* 2013). HAMC hydrogel intrathecal injection reduces inflammation in a rat model of spinal cord arachnoid inflammation (Austin *et al* 2012). As an additional measure to inhibit graft rejection, we pharmacologically suppressed the immune system of rats in our study. Anoikis can be triggered when anchorage-dependent cells are detached from their substrate for transplantation, especially into a cavity formed at the epicenter of a SCI. Transplantation of SKP-SCs in viscous hydrogels served the additional purpose of preventing anoikis by providing a polymer network for cell attachment. Further, SKP-SCs were grafted in a modified version of HAMC called eHAMC, where laminin- and fibronectin-derived peptide sequences were conjugated to MC. Laminin
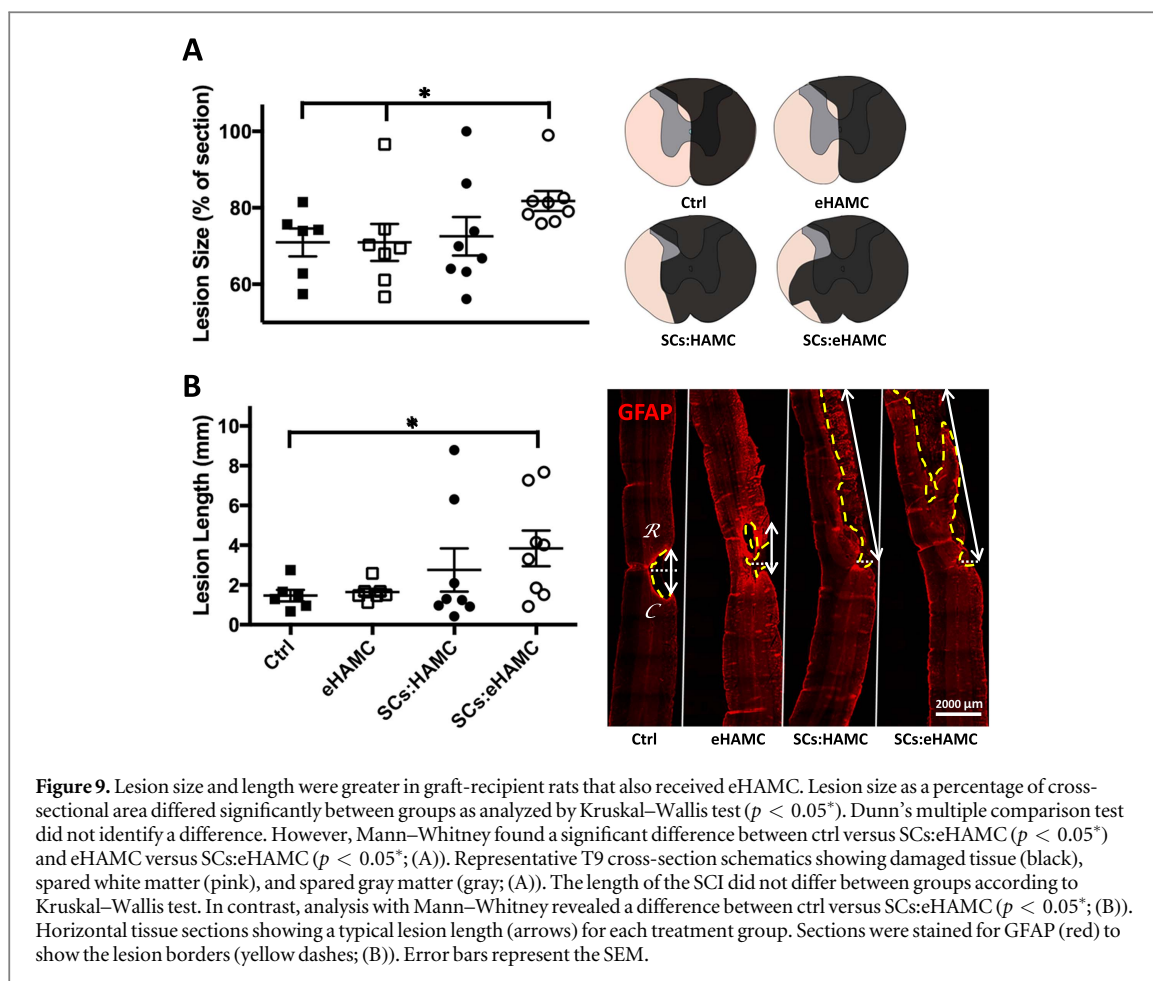
Figure 9. Lesion size and length were greater in graft-recipient rats that also received eHAMC. Lesion size as a percentage of cross-sectional area differed significantly between groups as analyzed by Kruskal–Wallis test ($p < 0.05^*$). Dunn's multiple comparison test did not identify a difference. However, Mann–Whitney found a significant difference between ctrl versus SCs:eHAMC ($p < 0.05^*$) and eHAMC versus SCs:eHAMC ($p < 0.05^*$; (A)). Representative T9 cross-section schematics showing damaged tissue (black), spared white matter (pink), and spared gray matter (gray; (A)). The length of the SCI did not differ between groups according to Kruskal–Wallis test. In contrast, analysis with Mann–Whitney revealed a difference between ctrl versus SCs:eHAMC ($p < 0.05^*$; (B)). Horizontal tissue sections showing a typical lesion length (arrows) for each treatment group. Sections were stained for GFAP (red) to show the lesion borders (yellow dashes; (B)). Error bars represent the SEM.
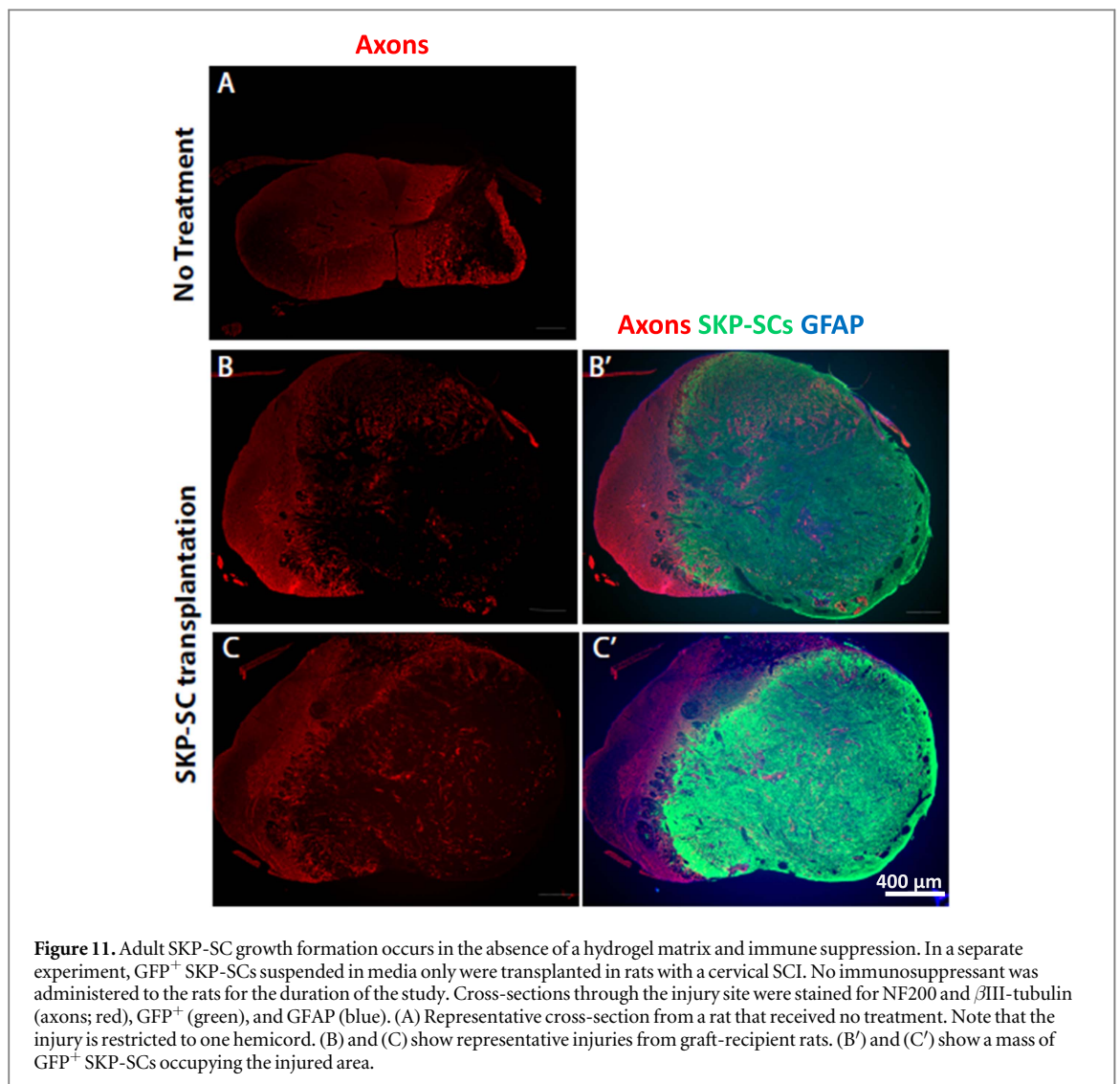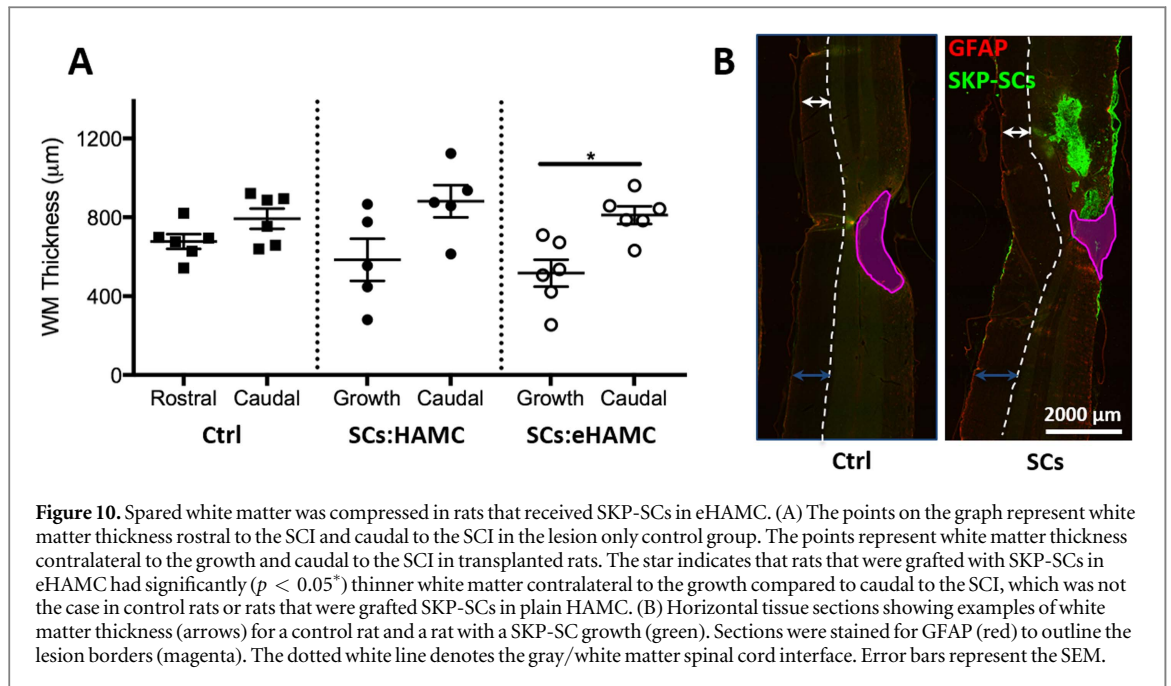
mediates SC attachment to substrata (Tohyama and Ide [1984](#)) and fibronectin promotes SC attachment and attracts SCs through chemotaxis (Baron-Van Evercooren *et al* [1982](#)). Hence, we predicted eHAMC would further reduce anoikis by promoting cell attachment compared to HAMC vehicle, resulting in improved filling of the cavity.

SKP-SCs survived when grafted in HAMC or eHAMC, showing both are supportive hydrogels for transplantation. The polymer network formed by hyaluronan (HA) and methylcellulose (MC) may be sufficient to stop anoikis and sustain cell viability. In fact, HA is a nonsulfated glycosaminoglycan found naturally in the ECM of nervous tissue (Vercruysse and Prestwich [1998](#)) that exists as a viscous liquid due to molecular entanglements between its long disaccharide polymers (Balazs [1991](#)). MC forms hydrophobic junctions thereby forming a gel (Schupper *et al* [2008](#)). The SKP-SCs could have interacted with the HA of HAMC via the CD44 transmembrane glycoprotein, which is expressed in high amounts in neonatal SCs and in varying amounts in adult SCs (Sherman *et al* [2000](#)). Possibly, this mechanical support provided by MC and molecular interactions with HA could have prevented anoikis, explaining why the addition of fibronectin and laminin peptide sequences to eHAMC had no further impact on cell survival. Alternatively, transformation of SKP-SCs to an oncogenic state

might have overridden the effect of eHAMC on cell survival. The purpose of the hydrogel in our study was to increase survival of grafted cells and to reduce the sinking of all cells to the ventral parts of the lesion. However, cells not only survived but proliferated, forming growths. This was also seen in a separate experiment (SKP-SCs in media), where no hydrogel was used. Thus, the hydrogel did not present an advantage.

The original goal of this study was to inject SKP-SCs into the SCI site with the intention of filling the cavity and forming a bridge for growing axons. However, SKP-SCs formed large growths in the spinal cord of the majority of grafted animals (SCs:HAMC 5 out of $n = 8$; SCs:eHAMC 6 out of $n = 8$). Given this alarming finding, the remainder of the discussion will focus on the oncogenic behavior of SKP-SCs in our study. SKP-SCs were found several mm rostral and caudal to the SCI site. This may have been the result of hyperproliferation of oncogenic SKP-SCs in the spinal cord, resulting in their expansion outside the injection site. Alternatively, oncogenic SKP-SCs may have migrated to other locations of the spinal cord through the spinal canal. Although rare, migration of spinal Schwannomas has previously been reported in humans (Khan *et al* [2013](#)).

The locomotor ability of two rats with SKP-SC growths (one from each cell transplantation group)

Figure 10. Spared white matter was compressed in rats that received SKP-SCs in eHAMC. (A) The points on the graph represent white matter thickness rostral to the SCI and caudal to the SCI in the lesion only control group. The points represent white matter thickness contralateral to the growth and caudal to the SCI in transplanted rats. The star indicates that rats that were grafted with SKP-SCs in eHAMC had significantly ($p < 0.05^*$) thinner white matter contralateral to the growth compared to caudal to the SCI, which was not the case in control rats or rats that were grafted SKP-SCs in plain HAMC. (B) Horizontal tissue sections showing examples of white matter thickness (arrows) for a control rat and a rat with a SKP-SC growth (green). Sections were stained for GFAP (red) to outline the lesion borders (magenta). The dotted white line denotes the gray/white matter spinal cord interface. Error bars represent the SEM.

Figure 11. Adult SKP-SC growth formation occurs in the absence of a hydrogel matrix and immune suppression. In a separate experiment, GFP$^+$ SKP-SCs suspended in media only were transplanted in rats with a cervical SCI. No immunosuppressant was administered to the rats for the duration of the study. Cross-sections through the injury site were stained for NF200 and βIII-tubulin (axons; red), GFP$^+$ (green), and GFAP (blue). (A) Representative cross-section from a rat that received no treatment. Note that the injury is restricted to one hemicord. (B) and (C) show representative injuries from graft-recipient rats. (B′) and (C′) show a mass of GFP$^+$ SKP-SCs occupying the injured area.

deteriorated markedly and suddenly. The rats lost the ability for weight supported plantar stepping in the span of 2 weeks. However, we did not see a group difference in locomotor function. This may be explained by the distribution of the growths. The masses differed in size, and were sometimes located unilaterally and sometimes bilaterally. It is known that even a small percentage of remaining white matter in the ventral funiculus is enough to support rhythmic hindlimb movements (BBB score 8; Schucht *et al* 2002). Therefore, it is not surprising that rats with large unilateral masses, such as #2 in figure 4, scored an average BBB score of 13. In other words, rat #2 could make coordinated weight-supported steps. In contrast, the rats that became paralyzed in a short span of time had bilateral growths, essentially making a complete SCI (rat from figure 3 and #1 from figure 4). Hence, obvious locomotor deterioration in a longer-term study would have depended on the directionality of the expansion of the growths. That is not to say that none of the other transplanted rats had motor deficits at the time of euthanasia. The applied open-field testing was probably not sensitive enough to detect subtle changes.

Lesion size analysis showed SCs:eHAMC rats had larger lesions compared to the lesion only control and HAMC vehicle groups. Further, spared white matter was compressed in SCs:eHAMC rats, which was not seen in SCs:HAMC rats or lesion only controls. These injuries were not due to the original SCIs, as they far exceeded a hemisection. Further evidence that cell grafts induced expansion of the injury comes from the finding that directly after injury (before cells were grafted) BBB scores were comparable between groups. Additionally, the lesion area corresponded to the spread of grafted cells. Thus, SKP-SC transplantation in eHAMC exacerbated the original SCI, deformed and possibly affected the function of initially spared tissue.

While growths were not restricted to the SCs:eHAMC group, the addition of laminin and fibronectin peptide sequences may have further increased SKP-SC mitotic activity. In fact, laminin is required for SC proliferation during development and provides a PI3-kinase/Akt-mediated survival signal (Yu 2005, Yu *et al* 2009), while fibronectin markedly stimulates rat SC proliferation in culture (Baron-Van Evercooren *et al* 1982). Hence, the advantages of attachment, survival, and growth-promoting factor inclusion in cell therapy vehicles should be weighed against the possibility of potentiating uncontrolled cell division. Furthermore, the addition of immune suppression interferes with endogenous mechanisms for detection and removal of oncogenic cells (Dressel *et al* 2008, Anderson *et al* 2011, Itakura *et al* 2015). Thus, it is possible immune suppression in our study prevented immune-mediated clearance of hyper-proliferative transplanted cells, permitting them to grow unchecked. However, it is important to immunosuppress animals receiving cell transplantation to

properly assess the risk of growth-formation. Indeed, immunosuppression of transplant-recipient animals in pre-clinical research has been recommended as standard practice for risk assessment (Anderson *et al* 2011).

The role of HAMC and cyclosporine in the formation of growths is clarified by the SKP-SCs in media study, performed without a hydrogel or immune suppressive agent. The results of the SKP-SCs in media study demonstrate that hyper-proliferation may occur in the absence of both factors. The inclusion of this experiment should not be viewed as a comparison to the SKP-SCs in hydrogel study, but as evidence that hyper-proliferation of SKP-SCs post-grafting is not an isolated event and may occur in a variety of conditions.

Further characterization of the phenotype of the transplanted cells revealed that the cell masses morphologically resembled Schwannomas. Schwannomas are nerve sheath tumors composed of bipolar SCs and are characterized by areas of hyper-cellularity (Antoni A bodies) and areas of hypo-cellularity (Antoni B bodies; Wippold *et al* 2007). Schwannoma immunohistochemistry markers include S100 protein, Leu 7-HNK 1 antigen, vimentin, GFAP, cytokeratin, laminin, heparan sulfate proteoglycan, fibronectin, and collagen (Guarino 1993). In the present study, transplanted GFP^+ SKP-SCs were primarily bipolar and organized into areas of hyper-cellularity (Antoni A) and hypo-cellularity (Antoni B; figure 6). Furthermore, transplanted GFP^+ SKP-SCs expressed S100 and fibronectin (figure 7). While large portions of GFP^+ SKP-SCs were not positive for S100, this could be attributed to malignant transformation of the Schwannomas. Typically, Schwannomas are benign growths but, in rare cases, undergo malignant transformation (Guccion and Enzinger 1979, Ducatman *et al* 1986, Lederman *et al* 1987, Vilanova *et al* 1998). Malignant Schwannomas often contain large numbers of S100 negative cells (Lederman *et al* 1987) and are associated with the predominance of hyper-cellularity (Ducatman *et al* 1986) and hemorrhage (Guccion and Enzinger 1979, Vilanova *et al* 1998). Hyper-cellularity and hemorrhage were two additional features seen in our study. Thus, SKP-SC growths in our study resembled malignant Schwannomas.

Notably, subset of GFP^+ cells did not express SC markers and appeared to take on a fibroblastic morphology, indicating that SKP-SCs may have adopted alternate fates within the injured spinal cord. Indeed, GFP^+ cells in our study expressed fibronectin, which is strongly expressed by fibroblasts (Stenman *et al* 1977, Baron-Van Evercooren *et al* 1982). It is also possible that the SKP-SCs acquired mutations in culture that prevented full maturation and allowed them to maintain an undifferentiated proliferative state leading to the exacerbated growths observed. Nestin and fibronectin are proteins expressed by SKPs (Fernandes *et al* 2004) and immature SCs in rodents (Jessen *et al* 1994, Dong *et al* 1999, Aquino *et al* 2006). Grafted

cells were positive for nestin and fibronectin, suggesting grafted cells were in an undifferentiated, immature state. Furthermore, grafted cells were positive for the proliferation antigen ki-67 (Gerdes *et al* 1984), confirming that grafted cells proliferated in the spinal cord.

Interestingly, neonatal mouse and rat SKP-SCs grown under identical conditions (with neuregulin and forskolin) to those in the present study never exhibited uncontrolled growth even after long-term transplantation (McKenzie *et al* 2006, Biernaskie *et al* 2007b, Kumar *et al* 2016), suggesting that adult SKP-SCs may be more susceptible to chromosomal aberration particularly during excessive cell division. This is consistent with reports that neonatal nerve-derived SCs 'aged' through extended expansion (>20 passages) acquire chromosomal abnormalities (Funk *et al* 2007). Our data here suggests that unlike neonatal cells, adult SKP-SCs undergo hastened transformation (5–10 passages) following extended culture in the presence of mitogens.

Further, propagation of large numbers of cells from a small starting pool, may inadvertently select for the cells that have acquired these proliferation-promoting mutations. Given that transformation of SKP-SCs is as prevalent with nerve-derived SCs exposed to parallel levels of expansion *in vitro*, there is no additional concern with SKP-derived relative to nerve-derived sources of SCs. Therefore, SKP-derived SCs remain a viable alternative source for SCs to repair the injured nervous system. Another factor that might have contributed to the oncogenic state of grafted cells is exposure to mycoplasma. After the experiment, frozen stock of GFP^+ lines 1 and 3 from the SKP-SCs in hydrogel study were thawed and tested for mycoplasma. The SKP-SCs thawed post hoc were mycoplasma positive. Thus, it is possible that GFP^+ SKP-SCs from cell lines 1 and 3 transplanted were contaminated with mycoplasma, impacting the reliability of our study. Mycoplasma has previously been reported to contribute to malignant transformation of mammalian cell types to a hyper-proliferative, oncogenic phenotype (Namiki *et al* 2009). However, our study does not provide a causal link between mycoplasma contamination and hyper-proliferation. Mycoplasma contamination is a variable that should be manipulated in future experiments to decipher the role of mycoplasma in growth-formation.

The present article highlights the vulnerability of adult SKP-SCs to transformation and importance of updating current cell culture strategies in pre-clinical research laboratories. We suggest that genetic indicators of transformation and incorporated suicide genes are not only applicable to pluripotent derivatives, but should also be considered for other proliferative progenitors, such as SKP-SCs, being used for cell therapy in order to improve safety for clinical trials. Ultimately, defining meticulous guidelines for culture expansion that preserve normal SKP-SC function and

that of other cell types will be important toward enabling safe and effective clinical translation.

Acknowledgments

ORCID iDs

Zacnicte May ⓘ https://orcid.org/0000-0003-0543-381X
Tobias Fuehrmann ⓘ https://orcid.org/0000-0003-1857-4806
Molly S Shoichet ⓘ https://orcid.org/0000-0003-1830-3475

References

Anderson A J, Haus D L, Hooshmand M J, Perez H, Sontag C J and Cummings B J 2011 Achieving stable human stem cell engraftment and survival in the CNS: is the future of regenerative medicine immunodeficient? *Regen. Med.* **6** 367–406

Aquino J B, Hjerling-Leffler J, Koltzenburg M, Edlund T, Villar M J and Ernfors P 2006 *In vitro* and *in vivo* differentiation of boundary cap neural crest stem cells into mature Schwann cells *Exp. Neurol.* **198** 438–49

Austin J W, Kang C E, Baumann M D, DiDiodato L, Satkunendrarajah K, Wilson J R and Fehlings M G 2012 The effects of intrathecal injection of a hyaluronan-based hydrogel on inflammation, scarring and neurobehavioural outcomes in a rat model of severe spinal cord injury associated with arachnoiditis *Biomaterials* **33** 4555–64

Balazs E A 1991 Medical applications of hyaluronan and its derivatives *Cosmetic Pharmaceutical Applications of Polymers* (New York: Plenum) pp 293–310

Balentine J D 1978 Pathology of experimental spinal cord trauma. I. The necrotic lesion as a function of vascular injury *Lab. Investigation* **39** 236–53

Ballios B G, Cooke M J, Donaldson L, Coles B L K, Morshead C M, van der Kooy D and Shoichet M S 2015 A hyaluronan-based injectable hydrogel improves the survival and integration of stem cell progeny following transplantation *Stem Cell Rep.* **4** 1031–45

Ballios B G, Cooke M J, van der Kooy D and Shoichet M S 2010 A hydrogel-based stem cell delivery system to treat retinal degenerative diseases *Biomaterials* **31** 2555–64

Bandtlow C, Zachleder T and Schwab M E 1990 Oligodendrocytes arrest neurite growth by contact inhibition *J. Neurosci.* **10** 3837–48

Barnett S C and Riddell J S 2004 Olfactory ensheathing cells (OECs) and the treatment of CNS injury: advantages and possible caveats *J. Anat.* **204** 57–67

Baron-Van Evercooren A, Kleinman H K, Seppä H E, Rentier B and Dubois-Dalcq M 1982 Fibronectin promotes rat Schwann cell growth and motility *J. Cell Biol.* **93** 211–6

Basso D M, Beattie M S and Bresnahan J C 1995 A sensitive and reliable locomotor rating scale for open field testing in rats *J. Neurotrauma* **12** 1–21

Biernaskie J, Sparling J S, Liu J, Shannon C P, Plemel J R, Xie Y and Tetzlaff W 2007a Skin-derived precursors generate myelinating Schwann cells that promote remyelination and functional recovery after contusion spinal cord injury *J. Neurosci.* **27** 9545–59

Biernaskie J A, McKenzie I A, Toma J G and Miller F D 2007b Isolation of skin-derived precursors (SKPs) and differentiation and enrichment of their Schwann cell progeny *Nat. Protocols* **1** 2803–12

Brederlau A, Correia A S, Anisimov S V, Elmi M, Paul G, Roybon L and Li J-Y 2006 Transplantation of human embryonic stem cell-derived cells to a rat model of parkinson's disease: effect of *in vitro* differentiation on graft survival and teratoma formation *Stem Cells* **24** 1433–40

Bunge R P 1975 Changing uses of nerve tissue culture 1950–1975 *The Nervous System* (*The Basic Neurosciences* vol 1) (New York: Raven Press) pp 31–42

Cafferty W B J, Duffy P, Huebner E and Strittmatter S M 2010 MAG and OMgp synergize with nogo-a to restrict axonal growth and neurological recovery after spinal cord trauma *J. Neurosci.* **30** 6825–37

Caicco M J, Zahir T, Mothe A J, Ballios B G, Kihm A J, Tator C H and Shoichet M S 2013 Characterization of hyaluronan-methylcellulose hydrogels for cell delivery to the injured spinal cord *J. Biomed. Mater. Res.* A **101** 1472–7

Chen M S, Huber A B, van der Haar M E, Frank M, Schnell L, Spillmann A A and Schwab M E 2000 Nogo-a is a myelin-associated neurite outgrowth inhibitor and an antigen for monoclonal antibody IN-1 *Nature* **403** 434–9

Choi D, Li D, Law S, Powell M and Raisman G 2008 A prospective observational study of the yield of olfactory ensheathing cells cultured from biopsies of septal nasal mucosa *Neurosurgery* **62** 1140–4

Choppa P, Vojdani A, Tagle C, Andrin R and Magtoto L 1998 Multiplex PCR for the detection of *Mycoplasma fermentans*, M. hominis and M. penetrans in cell cultures and blood samples of patients with chronic fatigue syndrome *Mol. Cell. Probes* **12** 301–8

Craig W S, Cheng S, Mullen D G, Blevitt J and Pierschbacher M D 1995 Concept and progress in the development of RGD-containing peptide pharmaceuticals *Biopolymers* **37** 157–75

Dong Z, Sinanan A, Parkinson D, Parmantier E, Mirsky R and Jessen K R 1999 Schwann cell development in embryonic mouse nerves *J. Neurosci. Res.* **56** 334–48

Dressel R, Schindehütte J, Kuhlmann T, Elsner L, Novota P, Baier P C and Mansouri A 2008 The tumorigenicity of mouse embryonic stem cells and *in vitro* differentiated neuronal cells is controlled by the recipients' immune response *PLoS One* **3** e2622

Ducatman B S, Scheithauer B W, Piepgras D G, Reiman H M and Ilstrup D M 1986 Malignant peripheral nerve sheath tumors. A clinicopathologic study of 120 cases *Cancer* **57** 2006–21

Enomoto M, Bunge M B and Tsoulfas P 2013 A multifunctional neurotrophin with reduced affinity to p75NTR enhances transplanted Schwann cell survival and axon growth after spinal cord injury *Exp. Neurol.* **248** 170–82

Fawcett J W and Asher R A 1999 The glial scar and central nervous system repair *Brain Res. Bull.* **49** 377–91

Feng S H, Tsai S, Rodriguez J and Lo S C 1999 Mycoplasmal infections prevent apoptosis and induce malignant transformation of interleukin-3-dependent 32D hematopoietic cells *Mol. Cell. Biol.* **19** 7995–8002

Fernandes K J L *et al* 2004 A dermal niche for multipotent adult skin-derived precursor cells *Nature Cell Biol.* **6** 1082–93

Flora G, Joseph G, Patel S, Singh A, Bleicher D, Barakat D J and Pearse D D 2013 Combining neurotrophin-transduced Schwann cells and rolipram to promote functional recovery from subacute spinal cord injury *Cell Transplant.* **22** 2203–17

Fouad K, Schnell L, Bunge M B, Schwab M E, Liebscher T and Pearse D D 2005 Combining Schwann cell bridges and olfactory-ensheathing glia grafts with chondroitinase promotes locomotor recovery after complete transection of the spinal cord *J. Neurosci.* **25** 1169–78

Franklin R J M and Barnett S C 1997 Do olfactory glia have advantages over Schwann cells for CNS repair? *J. Neurosci. Res.* **50** 665–72

Frisch S M and Francis H 1994 Disruption of epithelial cell-matrix interactions induces apoptosis *J. Cell Biol.* **124** 619–26

Führmann T, Tam R Y, Ballarin B, Coles B, Elliott Donaghue I, van der Kooy D and Shoichet M S 2016 Injectable hydrogel promotes early survival of induced pluripotent stem cell-derived oligodendrocytes and attenuates longterm teratoma formation in a spinal cord injury model *Biomaterials* **83** 23–36

Funakoshi H, Frisén J, Barbany G, Timmusk T, Zachrisson O, Verge V M and Persson H 1993 Differential expression of mRNAs for neurotrophins and their receptors after axotomy of the sciatic nerve *J. Cell Biol.* **123** 455–65

Funk D, Fricke C and Schlosshauer B 2007 Aging Schwann cells *in vitro Eur. J. Cell Biol.* **86** 207–19

Gerdes J, Lemke H, Baisch H, Wacker H H, Schwab U and Stein H 1984 Cell cycle analysis of a cell proliferation-associated human nuclear antigen defined by the monoclonal antibody Ki-67 *J. Immunology* **133** 1710–5

Golden K L, Pearse D D, Blits B, Garg M S, Oudega M, Wood P M and Bunge M B 2007 Transduced Schwann cells promote axon growth and myelination after spinal cord injury *Exp. Neurol.* **207** 203–17

Guarino M 1993 Plexiform Schwannoma, immunohistochemistry of Schwann cell markers, intermediate filaments and extracellular matrix components *Pathology—Res. Pract.* **189** 913–20

Guccion J G and Enzinger F M 1979 Malignant Schwannoma associated with von Recklinghausen's neurofibromatosis *Virchows Arch. Pathological Anat. Histology* **383** 43–57

Gupta D, Tator C H and Shoichet M S 2006 Fast-gelling injectable blend of hyaluronan and methylcellulose for intrathecal, localized delivery to the injured spinal cord *Biomaterials* **27** 2370–9

Hagg T and Oudega M 2006 Degenerative and spontaneous regenerative processes after spinal cord injury *J. Neurotrauma* **23** 264–80

Hagner A and Biernaskie J 2013 Isolation and differentiation of hair follicle-derived dermal precursors *Methods Mol. Biol.* **989** 247–63

Hannes V 2009 *Nervous System (Cambridge Illustrated Surgical Pathology)* ed L Weiss (New York: Cambridge University Press) (https://doi.org/10.1017/CBO9780511581076)

Hatae R, Miyazono M, Kohri R, Maeda K and Naito S 2014 Trochlear nerve Schwannoma with intratumoral hemorrhage presenting with persistent hiccups: a case report *J. Neurol. Surg. Rep.* **75** 183–8

Hill C E, Moon L D F, Wood P M and Bunge M B 2006 Labeled Schwann cell transplantation: cell loss, host Schwann cell replacement, and strategies to enhance survival *Glia* **53** 338–43

Itakura G, Kobayashi Y, Nishimura S, Iwai H, Takano M, Iwanami A and Nakamura M 2015 Controlling immune rejection is a fail-safe system against potential tumorigenicity after human iPSC-derived neural stem cell transplantation *PLoS One* **10** e0116413

Jeong J-O, Han J W, Kim J-M, Cho H-J, Park C, Lee N and Yoon Y-S 2011 Malignant tumor formation after transplantation of short-term cultured bone marrow mesenchymal stem cells in experimental myocardial infarction and diabetic neuropathy *Circ. Res.* **108** 1340–7

Jessen K R, Brennan A, Morgan L, Mirsky R, Kent A, Hashimoto Y and Gavrilovic J 1994 The Schwann cell precursor and its fate: a study of cell death and differentiation during gliogenesis in rat embryonic nerves *Neuron* **12** 509–27

Joannides A, Gaughwin P, Schwiening C, Majed H, Sterling J, Compston A and Chandran S 2004 Efficient generation of neural precursors from adult human skin: astrocytes promote neurogenesis from skin-derived stem cells *Lancet* **364** 172–8

Kawaja M D, Boyd J G, Smithson L J, Jahed A and Doucette R 2009 Technical strategies to isolate olfactory ensheathing cells for intraspinal implantation *J. Neurotrauma* **26** 155–77

Khan R A, Rahman A, Bhandari P B and Khan S K N 2013 Double migration of a Schwannoma of thoracic spine *Case Reports* (https://doi.org/10.1136/bcr-2012-008182)

Koda M, Someya Y, Nishio Y, Kadota R, Mannoji C, Miyashita T and Yamazaki M 2008 Brain-derived neurotrophic factor suppresses anoikis-induced death of Schwann cells *Neurosci. Lett.* **444** 143–7

Kontoveros D 2015 Schwann cell proliferation and migration in response to surface bound peptides for nerve regeneration *Master's Dissertation* OhioLINK, Electronic Theses and Dissertations Center (akron1431035725)

Kumar R, Sinha S, Hagner A, Stykel M, Raharjo E, Singh K K and Biernaskie J 2016 Adult skin-derived precursor Schwann cells exhibit superior myelination and regeneration supportive properties compared to chronically denervated nerve-derived Schwann cells *Exp. Neurol.* **278** 127–42

Langford L A, Porter S and Bunge R P 1988 Immortalized rat Schwann cells produce tumours *in vivo J. Neurocytology* **17** 521–9

Lederman S M, Martin E C, Laffey K T and Lefkowitch J H 1987 Hepatic neurofibromatosis, malignant Schwannoma, and angiosarcoma in von Recklinghausen's disease *Gastroenterology* **92** 234–9

Lee J H, Streijger F, Tigchelaar S, Maloon M, Liu J, Tetzlaff W and Kwon B K 2012 A contusive model of unilateral cervical spinal cord injury using the infinite horizon impactor *J. Visualized Exp.* **65** 3313

McKenzie I A, Biernaskie J, Toma J G, Midha R and Miller F D 2006 Skin-derived precursors generate myelinating Schwann cells for the injured and dysmyelinated nervous system *J. Neurosci.* **26** 6651–60

Meier C, Parmantier E, Brennan A, Mirsky R and Jessen K R 1999 Developing Schwann cells acquire the ability to survive without axons by establishing an autocrine circuit involving insulin-like growth factor, neurotrophin-3, and platelet-derived growth factor-BB *J. Neurosci.* **19** 3847–59

Meyer M, Matsuoka I, Wetmore C, Olson L and Thoenen H 1992 Enhanced synthesis of brain-derived neurotrophic factor in the lesioned peripheral nerve: different mechanisms are responsible for the regulation of BDNF and NGF mRNA *J. Cell Biol.* **119** 45–54

Morrissey T K, Kleitman N and Bunge R P 1991 Isolation and functional characterization of Schwann cells derived from adult peripheral nerve *J. Neurosci.* **11** 2433–42

Mothe A J, Tam R Y, Zahir T, Tator C H and Shoichet M S 2013 Repair of the injured spinal cord by transplantation of neural stem cells in a hyaluronan-based hydrogel *Biomaterials* **34** 3775–83

Murray M R and Stout A P 1942 Characteristics of human Schwann cells *in vitro Anatomical Rec.* **84** 275–93

Namiki K, Goodison S, Porvasnik S, Allan R W, Iczkowski K A, Urbanek C and Rosser C J 2009 Persistent exposure to mycoplasma induces malignant transformation of human prostate cells *PLoS One* **4** e6872

National Spinal Cord Injury Statistical Center 2016 *Spinal Cord Injury (SCI) Facts and Figures at a Glance* (Birmingham, AL: University of Alabama at Birmingham)

Oudega M, Bradbury E J and Ramer M S 2012 Combination therapies *Handbook of Clinical Neurology* vol 109 (Amsterdam: Elsevier) pp 617–36

Oudega M and Xu X-M 2006 Schwann cell transplantation for repair of the adult spinal cord *J. Neurotrauma* **23** 453–67

Pearse D D, Pereira F C, Marcillo A E, Bates M L, Berrocal Y A, Filbin M T and Bunge M B 2004 cAMP and Schwann cells promote axonal growth and functional recovery after spinal cord injury *Nat. Med.* **10** 610–6

Pearse D D, Sanchez A R, Pereira F C, Andrade C M, Puzis R, Pressman Y and Bunge M B 2007 Transplantation of Schwann cells and/or olfactory ensheathing glia into the contused spinal cord: survival, migration, axon association, and functional recovery *Glia* **55** 976–1000

Rahmani W, Abbasi S, Hagner A, Raharjo E, Kumar R, Hotta A and Biernaskie J 2014 Hair follicle dermal stem cells regenerate the dermal sheath, repopulate the dermal papilla, and modulate hair type *Dev. Cell* **31** 543–58

Richardson P M, McGuinness U M and Aguayo A J 1980 Axons from CNS neurons regenerate into PNS grafts *Nature* **284** 264–5

Richner M, Ulrichsen M, Elmegaard S L, Dieu R, Pallesen L T and Vaegter C B 2014 Peripheral nerve injury modulates neurotrophin signaling in the peripheral and central nervous system *Mol. Neurobiol.* **50** 945–70

Rodriguez F J, Folpe A L, Giannini C and Perry A 2012 Pathology of peripheral nerve sheath tumors: diagnostic overview and update on selected diagnostic problems *Acta Neuropathologica* **123** 295–319

Safety of Autologous Human Schwann Cells (ahSC) in Subjects with Subacute SCI (Identification No. NCT01739023) (2012), retrieved from clinicaltrials.gov

Sahenk Z, Oblinger J and Edwards C 2008 Neurotrophin-3 deficient Schwann cells impair nerve regeneration *Exp. Neurol.* **212** 552–6

Schucht P, Raineteau O, Schwab M E and Fouad K 2002 Anatomical correlates of locomotor recovery following dorsal and ventral lesions of the rat spinal cord *Exp. Neurol.* **176** 143–53

Schupper N, Rabin Y and Rosenbluh M 2008 Multiple stages in the aging of a physical polymer gel *Macromolecules* **41** 3983–94

Sharp K G, Flanagan L A, Yee K M and Steward O 2012 A re-assessment of a combinatorial treatment involving Schwann cell transplants and elevation of cyclic AMP on recovery of motor function following thoracic spinal cord injury in rats *Exp. Neurol.* **233** 625–44

Sherman L S, Rizvi T A, Karyala S and Ratner N 2000 CD44 enhances neuregulin signaling by Schwann cells *J. Cell Biol.* **150** 1071–84

Sparling J S, Bretzner F, Biernaskie J, Assinck P, Jiang Y, Arisato H and Tetzlaff W 2015 Schwann cells generated from neonatal skin-derived precursors or neonatal peripheral nerve improve functional recovery after acute transplantation into the partially injured cervical spinal cord of the rat *J. Neurosci.* **35** 6714–30

Stenman S, Wartiovaara J and Vaheri A 1977 Changes in the distribution of a major fibroblast protein, fibronectin, during mitosis and interphase *J. Cell Biol.* **74** 453–67

Tai C, Miscik C L, Ungerer T D, Roppolo J R and de Groat W C 2006 Suppression of bladder reflex activity in chronic spinal cord injured cats by activation of serotonin 5-HT1A receptors *Exp. Neurol.* **199** 427–37

Tam R Y, Cooke M J and Shoichet M S 2012 A covalently modified hydrogel blend of hyaluronan-methyl cellulose with peptides and growth factors influences neural stem/progenitor cell fate *J. Mater. Chem.* **22** 19402

Tetzlaff W, Okon E B, Karimi-Abdolrezaee S, Hill C E, Sparling J S, Plemel J R and Kwon B K 2011 A systematic review of cellular transplantation therapies for spinal cord injury *J. Neurotrauma* **28** 1611–82

The Safety of ahSC in Chronic SCI With Rehabilitation (Identification No. NCT02354625 (2015), retrieved from clinicaltrials.gov

Thor K B, Roppolo J R and deGroat W C 1983 Naloxone induced micturition in unanesthetized paraplegic cats *J. Urology* **129** 202–5

Thuret S, Moon L D F and Gage F H 2006 Therapeutic interventions after spinal cord injury *Nat. Rev. Neurosci.* **7** 628–43

Tohyama K and Ide C 1984 The localization of laminin and fibronectin on the Schwann cell basal lamina *Arch. Histology Cytology* **47** 519–32

Toma J G, Akhavan M, Fernandes K J, Barnabé-Heider F, Sadikot A, Kaplan D R and Miller F D 2001 Isolation of multipotent adult stem cells from the dermis of mammalian skin *Nat. Cell Biol.* **3** 778–84

Toma J G, McKenzie I A, Bagli D and Miller F D 2005 Isolation and characterization of multipotent skin-derived precursors from human skin *Stem Cells* **23** 727–37

Tsai S, Wear D J, Shih J W and Lo S C 1995 Mycoplasmas and oncogenesis: persistent infection and multistage malignant transformation *Proc. Natl Acad. Sci. USA* **92** 10197–201

US National Library of Medicine (2 April 2017), Clinical trials.gov: A service of the US National Institutes of Health, retrieved from clinicaltrials.gov

Vercruysse K P and Prestwich G D 1998 Hyaluronate derivatives in drug delivery *Crit. Rev. Therapeutic Drug Carrier Syst.* **15** 513–55

Vilanova J C, Dolz J L, Maestro de Leon J L, Aparicio A, Aldomà J and Capdevila A 1998 MR imaging of a malignant Schwannoma and an osteoblastoma with fluid-fluid levels. Report of two new cases *Eur. Radiol.* **8** 1359–62

Vroemen M and Weidner N 2003 Purification of Schwann cells by selection of p75 low affinity nerve growth factor receptor expressing cells from adult peripheral nerve *J. Neurosci. Methods* **124** 135–43

Wang K C, Koprivica V, Kim J A, Sivasankaran R, Guo Y, Neve R L and He Z 2002 Oligodendrocyte-myelin glycoprotein is a Nogo receptor ligand that inhibits neurite outgrowth *Nature* **417** 941–4

Watson C, Paxinos G, Kayalioglu G and Heise C 2009 Atlas of the rat spinal cord *The Spinal Cord* (Amsterdam: Elsevier) pp 238–306

Whishaw I Q, Gorny B and Sarna J 1998 Paw and limb use in skilled and spontaneous reaching after pyramidal tract, red nucleus and combined lesions in the rat: behavioral and anatomical dissociations *Behav. Brain Res.* **93** 167–83

Williams R R, Henao M, Pearse D D and Bunge M B 2015 Permissive Schwann cell graft/spinal cord interfaces for axon regeneration *Cell Transplant.* **24** 115–31

Wippold F J, Lubner M, Perrin R J, Lämmle M and Perry A 2007 Neuropathology for the neuroradiologist: Antoni A and Antoni B tissue patterns *Am. J. Neuroradiol.* **28** 1633–8

Xu X-M and Onifer S M 2009 Transplantation-mediated strategies to promote axonal regeneration following spinal cord injury *Respiratory Physiol. Neurobiol.* **169** 171–82

Yu W-M 2005 Schwann cell-specific ablation of laminin 1 causes apoptosis and prevents proliferation *J. Neurosci.* **25** 4463–72

Yu W-M, Chen Z-L, North A J and Strickland S 2009 Laminin is required for Schwann cell morphogenesis *J. Cell Sci.* **122** 929–36

Zheng J, Kontoveros D, Lin F, Hua G, Reneker D H, Becker M L and Willits R K 2015 Enhanced Schwann cell attachment and alignment using one-pot 'dual click' GRGDS and YIGSR derivatized nanofibers *Biomacromolecules* **16** 357–63